Planet Simulator

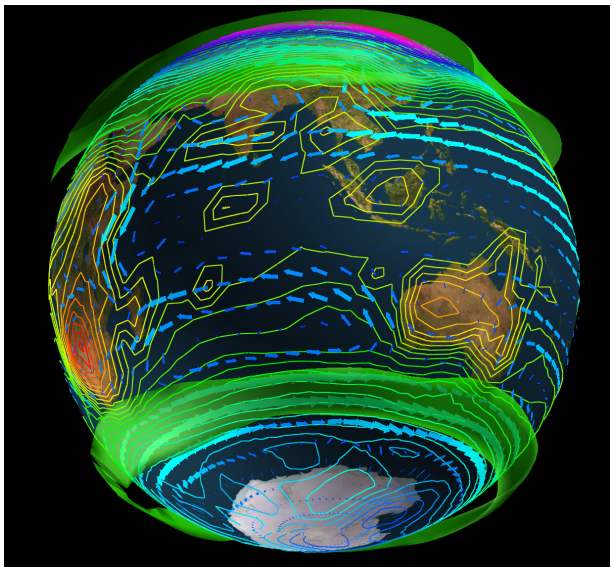

Reference Manual

Version 16

F. Lunkeit H. Borth M. Böttinger K. Fraedrich H. Jansen
E. Kirk A. Kleidon U. Luksch P. Paiewonsky S. Schubert
S. Sielmann H. Wan

February 6, 2012

Contents

Chapter 1

Preface

For two decades, a comprehensive, three-dimensional global atmospheric general circulation model (GCM) is being provided by the National Center for Atmospheric Research (NCAR, Climate and Global Dynamics Division) to university and other scientists for use in analysing and understanding the global climate. Designed as a Community Climate Model (CCM) it has been continuously developed since. Other centres have also constructed comprehensive climate models of similarly high complexity, mostly for their research interests.

As the complexity of general circulation models has been and still is growing considerably, it is not surprising that, for both education and research, models simpler than those comprehensive GCMs at the cutting edge of the development, are becoming more and more attractive. These medium complexity models do not simply enhance the climate model hierarchy. They support understanding atmospheric or climate phenomena by simplifying the system gradually to reveal the key mechanisms. They also provide an ideal tool kit for students to be educated and to teach themselves, gaining practice in model building or modeling. Our aim is to provide such a model of intermediate complexity for the university environment: the PlanetSimulator. It can be used for training the next GCM developers, to support scientists to understand climate processes, and to do fundamental research.

From PUMA to PlanetSimulator: Dynamical core and physical processes comprise a general circulation model (GCM) of planetary atmospheres. Stand-alone, the dynamical core is a simplified general circulation model like our Portable University Model of the Atmosphere or PUMA. Still, linear processes are introduced to run it, like Newtonian cooling and Rayleigh friction, which parameterise diabatic heating and planetary boundary layers. Though simple, PUMA has been enjoying a wide spectrum of applications and initiating collaborations in fundamental research, atmospheric dynamics and education alike. Specific applications, for example, are tests and consequences of the maximum entropy production principle, synchronisation and spatio-temporal coherence resonance, large scale dynamics of the atmospheres on Earth, Mars and Titan. Based on this experience we combined the leitmotifs behind PUMA and the Community Model, to applying, building, and coding a 'PlanetSimulator'.

Applying the PlanetSimulator in a university environment has two aspects: First, the code must be open and freely available as the software required to run it; it must be user friendly, inexpensive and equipped with a graphical user interface. Secondly, it should be suitable for teaching project studies in classes or lab, where students practice general circulation modelling, in contrast to technicians running a comprehensive GCM; that is, science versus engineering.

Building the PlanetSimulator includes, besides an atmospheric GCM of medium complexity, other compartments of the climate system, for example, an ocean with sea ice, a land surface with biosphere. Here these other compartments are reduced to linear systems. That is, not unlike PUMA as a dynamical core with linear physics, the PlanetSimulator consists of a GCM with, for example, a linear ocean/sea-ice module formulated in terms of a mixed layer energy

balance. The soil/biosphere module is introduced analoguously. Thus, working the Planet-Simulator is like testing the performance of an atmospheric or oceanic GCM interacting with various linear processes, which parameterise the variability of the subsystems in terms of their energy (and mass) balances.

Coding the PlanetSimulator requires that it is portable to many platforms ranging from personal computers over workstations to mainframes; massive parallel computers and clusters of networked machines are also supported. The system is scalable with regard to vertical and horizontal resolutions, provides experiment dependent model configurations, and it has a transparent and rich documented code.

Acknowledgement: The development of the Planet Simulator was generously granted by the German Federal Ministry for Education and Research (BMBF) during the years 2000 - 2003.

Part I

Atmosphere: Wet Primitive Equations

Chapter 2

Model Dynamics

The primitive equations, which represent the dynamical core of the atmospheric model, consist of the conservation of momentum and mass, the first law of thermodynamics and the equation of state, simplified by the hydrostatic approximation.

2.1 A dimensionless set of differential equations

The prognostic equations for the horizontal velocities are transformed into equations of the vertical component of the vorticity ζ and the divergence D. A vertical coordinate system where the lower boundary exactly coincides with a coordinate surface is defined by σ (the pressure normalized by the surface pressure). Latitude φ and longitude λ represent the horizontal coordinates and the poleward convergence of the meridians is explicitly introduced re-writing the zonal (u) and meridional (ν) velocities: $U = u\cos\varphi$, $V = \nu\cos\varphi$ and $\mu = \sin\varphi$. The implicitly treated gravity wave terms are linearized about a reference profile T_0. Therefore, prognostic equation for temperature deviations $T' = T - T_0$ are derived; we use a constant reference temperature $T_0 = 250K$ for all σ levels. The turbulent flux divergences due to prior Reynolds averaging enter the dynamic and thermodynamic equations as parameterizations formally included in the terms: P_ζ, P_D, P_T.

A dimensionless set of differential equations is derived by scaling vorticity ζ and divergence D by angular velocity of the earth Ω, pressure p by a constant surface pressure p_s, temperatures T and T' by $a^2\Omega^2/R$ and the orography and geopotential ψ by $a^2\Omega^2/g$ (g is the acceleration of gravity and R the gas constant for dry air). The dimensionless primitive equations in the (λ, μ, σ)-coordinates [Hoskins and Simmons (1975)] are given by

Conservation of momentum (vorticity and divergence equation)

$$\frac{\partial\zeta + f}{\partial t} = \frac{1}{(1-\mu^2)}\frac{\partial F_\nu}{\partial\lambda} - \frac{\partial F_u}{\partial\mu} + P_\zeta \tag{2.1}$$

$$\frac{\partial D}{\partial t} = \frac{1}{(1-\mu^2)}\frac{\partial F_u}{\partial\lambda} + \frac{\partial F_\nu}{\partial\mu} - \bigtriangledown^2 E - \bigtriangledown^2(\phi + T_0\ln p_s) + P_D \tag{2.2}$$

Hydrostatic approximation (using the equation of state)

$$0 = \frac{\partial\phi}{\partial\ln\sigma} + T \tag{2.3}$$

Conservation of mass (continuity equation)

$$\frac{\partial \ln p_s}{\partial t} = -\int_0^1 A d\sigma \tag{2.4}$$

Thermodynamic equation

$$\frac{\partial T'}{\partial t} = F_T - \dot{\sigma}\frac{\partial T}{\partial \sigma} + \kappa W T + \frac{J}{c_p} + P_T \tag{2.5}$$

with the notations

$$F_u = (\zeta + f)V - \dot{\sigma}\frac{\partial U}{\partial \sigma} - T'\frac{\partial \ln p_s}{\partial \lambda}$$
$$F_\nu = -(\zeta + f)U - \dot{\sigma}\frac{\partial V}{\partial \sigma} - (1-\mu^2)T'\frac{\partial \ln p_s}{\partial \mu}$$
$$F_T = -\frac{1}{(1-\mu^2)}\frac{\partial (UT')}{\partial \lambda} - \frac{\partial (VT')}{\partial \mu} + DT'$$
$$E = \frac{U^2 + V^2}{2(1-\mu^2)}$$
$$\dot{\sigma} = \sigma \int_0^1 A d\sigma - \int_0^\sigma A d\sigma$$
$$W = \frac{\omega}{p} = \vec{V}\cdot\nabla \ln p_s - \frac{1}{\sigma}\int_0^\sigma A d\sigma$$
$$A = D + \vec{V}\cdot\nabla \ln p_s = \tfrac{1}{p_s}\nabla \cdot p_s \vec{V}.$$

Here is $\dot{\sigma}$ the vertical velocity in the σ system, J the diabatic heating per unit mass and E the kinetic energy per unit mass. The streamfunction ψ and the velocity potential χ represent the nondivergent and the irrotational part of the velocity field
$U = -(1-\mu^2)\frac{\partial \psi}{\partial \mu} + \frac{\partial \chi}{\partial \lambda}$ and $V = \frac{\partial \psi}{\partial \lambda} + (1-\mu^2)\frac{\partial \chi}{\partial \mu}$ with $\zeta = \nabla^2\psi$ and $D = \nabla^2\chi$.

2.2 Mode splitting

The fast gravity wave modes are linearized around a reference temperature profile $\vec{T_0}$. Now, the differential equations (2.1-2.5) can be separated into fast (linear) gravity modes and the slower non-linear terms (N_D, N_p, N_T). The linear terms of the equations contain the effect of the divergence (or the gravity waves) on the surface pressure tendency, the temperature tendency and the geopotential. A discussion of the impact of the reference profile on the stability of the semi-implicit numerical scheme is presented by [Simmons et al.(1978)].

$$\frac{\partial D}{\partial t} = N_D - \bigtriangledown^2(\phi + T_0 \ln p_s) \tag{2.6}$$

$$\frac{\partial \phi}{\partial \ln \sigma} = -T \tag{2.7}$$

$$\frac{\partial \ln p_s}{\partial t} = N_p - \int_0^1 D d\sigma \tag{2.8}$$

$$\frac{\partial T'}{\partial t} = N_T - \dot{\sigma}_L \frac{\partial T_0}{\partial \sigma} + \kappa W_L T_0 \tag{2.9}$$

with the non-linear terms

$$N_D = \frac{1}{(1-\mu^2)} \frac{\partial F_u}{\partial \lambda} + \frac{F_\nu}{\partial \mu} - \bigtriangledown^2 E + P_D$$

$$N_p = -\int_0^1 [A - D] d\sigma$$

$$N_T = F_T - \dot{\sigma}_N \frac{\partial T_0}{\partial \sigma} - \dot{\sigma} \frac{\partial T'}{\partial \sigma} + \kappa W_N T_0 + \kappa W T' + \frac{J}{c_p} + P_T$$

and the notations

$$\dot{\sigma}_L = \sigma \int_0^1 D d\sigma - \int_0^\sigma D d\sigma$$

$$\dot{\sigma}_N = \sigma \int_0^1 [A - D] d\sigma - \int_0^\sigma [A - D] d\sigma$$

$$W_L = -\frac{1}{\sigma} \int_0^\sigma D d\sigma$$

$$W_N = \vec{V} \cdot \nabla \ln p_s - \frac{1}{\sigma} \int_0^\sigma [A - D] d\sigma$$

$$A - D = \vec{V} \cdot \nabla \ln p_s$$

$$\dot{\sigma} = \dot{\sigma_L} + \dot{\sigma_N} = \sigma \int_0^1 A d\sigma - \int_0^\sigma A d\sigma$$

$$W = W_L + W_N = \vec{V} \cdot \nabla \ln p_s - \frac{1}{\sigma} \int_0^\sigma A d\sigma$$

The index L denote the linear and N the non-linear part in the vertical advection ($\dot{\sigma} \frac{\partial T}{\partial \sigma}$) and the adiabatic heating or cooling ($\kappa W T$ with $W = \frac{\omega}{p}$). The non-linear terms are solve explicitly in the physical space (on the Gaussian grid; section 2.3.1) and the linear terms are calculated implicitly in the spectral space (for the spherical harmonics; see section 2.3.1).

2.3 Numerics

Solving the equations requires a suitable numerical representation of the spatial fields and their time change. A conventional approach is spectral representation in the horizontal using the transform method, finite differences in the vertical, and a semi-implicit time stepping.

2.3.1 Spectral Transform method

The spectral method used in the computation of the nonlinear terms involves storing of a large number of so-called interaction coefficients, the number of which increases very fast with increasing resolution. The computing time and storing space requirements exceed all practical limits for high resolution models. Furthermore, there are problems to incorporate locally dependent physical processes, such as release of precipitation or a convective adjustment. Therefore, the equations are solved using the spectral transform method [Orszag (1970), Eliassen et al. (1970)]. This method uses an auxiliary grid in the physical space where point values of the dependent variables are computed.

The prognostic variables are represented in the horizontal by truncated series of spherical harmonics (Q stands for ζ, D, T and $\ln p_s$)

$$Q(\lambda,\mu,\sigma,t) = \sum_{m=-M}^{M} \sum_{n=|m|}^{M} Q_n^m(\sigma,t) P_n^m(\mu) e^{im\lambda} \tag{2.10}$$

$$= Q_n^0(\sigma,t)P_n^0(\mu) + 2\sum_{m=1}^{M}\sum_{n=m}^{M} Q_n^m(\sigma,t)P_n^m(\mu)e^{im\lambda}$$

For each variable the spectral coefficient is defined by

$$Q_n^m(\sigma,t) = \frac{1}{4\pi}\int_{-1}^{1}\int_{0}^{2\pi} Q(\lambda,\mu,\sigma,t)P_n^m(\mu)e^{-im\lambda}d\lambda d\mu \tag{2.11}$$

The spectral coefficients $Q_n^m(\sigma,t)$ are obtained by Gaussian quadrature of the Fourier coefficients F^m at each latitude φ which are calculated by Fast Fourier Transformation with

$$F^m(\mu,\sigma,t) = \frac{1}{4\pi}\int_{0}^{2\pi} Q(\lambda,\mu,\sigma,t)e^{-im\lambda}d\lambda$$

The auxiliary grid in the physical space (Gaussian grid) is defined by M_g equally spaced longitudes and J_g Gaussian latitudes with $M_g \geq 3M+1$ and $J_g \geq 0.5(3M+1)$.

2.3.2 Vertical discretization

The prognostic variables vorticity, temperature and divergence are calculated at full levels and the vertical velocity at half levels. Therefore, the vertical advection for the level r is calculated (Q stands for ζ, D, T and $\ln p_s$)

$$(\dot\sigma\frac{\partial Q}{\partial\sigma})\hat{=}\frac{1}{2\Delta\sigma_r}[\dot\sigma_{r+0.5}(Q_{r+1}-Q_r)+\dot\sigma_{r-0.5}(Q_r-Q_{r-1})] \tag{2.12}$$

For the hydrostatic approximation (3) an angular momentum conserving finite-difference scheme [Simmons and Burridge (1981)] is used which solves the equation at half levels ($r+0.5; r=1,...,n; n=$ number of levels)

$$\frac{\partial\phi}{\partial\ln\sigma} + T\hat{=}\phi_{r+0.5}-\phi_{r-0.5}+T_r\cdot\ln\frac{\sigma_{r+0.5}}{\sigma_{r-0.5}} \tag{2.13}$$

Full level values (r) of geopotential are given by

$$\phi_r = \phi_{r+0.5} + \alpha_r T_r \tag{2.14}$$

with $\alpha_r = 1 - \frac{\sigma_{r-0.5}}{\Delta\sigma_r}\ln\frac{\sigma_{r+0.5}}{\sigma_{r-0.5}}$ and $\Delta\sigma_r = \sigma_{r+0.5}-\sigma_{r-0.5}$

2.3.3 Semi-implicit time stepping

Sound waves are filtered by the hydrostatic approximation (filter for vertical sound waves) and the lower boundary condition in pressure or sigma-coordinates (vanishing vertical velocity at the surface, i.e. the total derivative of the surface pressure is zero; filter for horizontal sound waves). But the fast propagation of the gravity waves strongly reduce the time step of explicit numerical schemes, therefore mode splitting is used (section 2.2) and an implicit scheme for the divergence is applied (see below). The vorticity equation is computed by an explicit scheme (leap frog) and the common Robert/Asselin time filter is used [Haltiner and Williams (1982)].

The implicit formulation for the divergence is derived using the conservation of mass, the hydrostatic approximation and the thermodynamic equation (eq. 2.6-2.9) approximated by its finite difference analogues in time (t) using the notation (for each variable D, T, $\ln p_s$, and ϕ)

$$\delta_t Q = \frac{Q^{t+\Delta t} - Q^{t-\Delta t}}{2\Delta t} \qquad \text{and} \qquad \overline{Q}^t = 0.5(Q^{t+\Delta t} + Q^{t-\Delta t}) = Q^{t-\Delta t} + \Delta t \delta_t Q$$

The divergence is calculated by the non-linear term at time step t and the linearized term which is a function of the geopotential (or the temperature tendency) and the surface pressure tendency.

$$\delta_t D = {N_D}^t - \bigtriangledown^2(\overline{\phi}^t + T_0[\ln p_s^{t-\Delta t} + \Delta t\ \delta_t \ln p_s]) \tag{2.15}$$

$$\overline{\phi - \phi_s}^t = L_\phi[T^{t-\Delta t} + \Delta t \delta_t T] = L_\phi[T^{t-\Delta t} + \Delta t\ \delta_t T'] \tag{2.16}$$

$$\delta_t \ln p_s = {N_p}^t - L_p[D^{t-\Delta t} + \Delta t\ \delta_t D] \tag{2.17}$$

$$\delta_t T' = {N_T}^t - L_T[D^{t-\Delta t} + \Delta t\ \delta_t D] \tag{2.18}$$

The implicit formulation of the divergence equation is derived from the finite difference analogues of the new time step $t + \Delta t$ applied for each level r ($r = 1, ...n$) which can also formulated as a vector $\vec{D}$ with the n components.

$$\begin{pmatrix} 1 - b_{11} & b_{21} & \cdots & b_{n1} \\ b_{12} & 1 - b_{22} & \ddots & \vdots \\ \vdots & \vdots & \ddots & \vdots \\ b_{1n} & b_{2n} & \cdots & 1 - b_{nn} \end{pmatrix} \begin{pmatrix} D_1^{t+\Delta t} \\ D_2^{t+\Delta t} \\ \vdots \\ D_n^{t+\Delta t} \end{pmatrix} = \begin{pmatrix} D_1^{t-\Delta t} \\ D_2^{t-\Delta t} \\ \vdots \\ D_n^{t-\Delta t} \end{pmatrix} + 2\Delta t \begin{pmatrix} R_1 \\ R_2 \\ \vdots \\ R_n \end{pmatrix}$$

In matrix formulation

$$(\mathcal{I} - \mathcal{B}\Delta t^2 \bigtriangledown^2)\vec{D}^{t+\Delta t} = \vec{D}^{t-\Delta t} + 2\Delta t[\vec{N}_D - \bigtriangledown^2(\vec{\phi}^{t-\Delta t} + \vec{T}_0 \ln p_s^{t-\Delta t})]$$

$$-2\Delta t^2 \bigtriangledown^2 (\mathcal{L}_\phi \vec{N}_T + \vec{T}_0 N_p) \tag{2.19}$$

The matrix $\mathcal{B} = \mathcal{L}_\phi \mathcal{L}_T + \vec{T}_0 \vec{L}_p = \mathcal{B}(\sigma, \kappa, \vec{T}_0)$ is constant in time. The variables $\vec{D}, \vec{T}, \vec{T}', \vec{\phi} - \vec{\phi}_s$ are represented by column vectors with values at each layer, as are also $\vec{N}_D$ and $\vec{N}_T$. $\mathcal{L}_\phi$ and $\mathcal{L}_T$ are constant matrices, $\vec{L}_p$ is a row vector (see Appendix C). The matrix $\mathcal{B}$ can be calculated

seperately for each spectral coefficient because in the linearized part the spectral modes are independent of each other.

$$(\vec{D}_n^m)^{t+\Delta t} = (\mathcal{I} + \mathcal{B}\Delta t^2 c_n)^{-1}[(\vec{D}_n^m)^{t-\Delta t} + 2\Delta t\vec{R}] \tag{2.20}$$

$$(\vec{D}_n^m)^{t+\Delta t} = (\frac{\mathcal{I}}{c_n} + \mathcal{B}\Delta t^2)^{-1}[\frac{1}{c_n}(\vec{D}_n^m)^{t-\Delta t} + \frac{2\Delta t}{c_n}\vec{R}] \tag{2.21}$$

with $\bigtriangledown^2(P_n^m(\mu)e^{-im\lambda}) = -n(n+1)P_n^m(\mu)e^{-im\lambda} = -c_n P_n^m(\mu)e^{-im\lambda}$.

Chapter 3

Model Physics - Parameterizations

3.1 Surface Fluxes and Vertical Diffusion

3.1.1 Surface Fluxes

The bulk aerodynamic formulas are used to parameterize surface fluxes of zonal and meridional momentum (wind stress) F_u and F_v, sensible heat F_T and latent heat $L\,F_q$, where F_q is the surface flux of moisture and L is the latent heat of vaporisation L_v, or, depending on temperature, the latent heat of sublimation L_s:

$$\begin{aligned} F_u &= \rho\, C_m\, |\vec{v}|\, u \\ F_v &= \rho\, C_m\, |\vec{v}|\, v \\ F_T &= c_p\, \rho\, C_h\, |\vec{v}|\, (\gamma T - T_S) \\ L\, F_q &= L\, \rho\, C_h\, C_w\, |\vec{v}|\, (\delta q - q_S) \end{aligned} \tag{3.1}$$

All fluxes are positive in downward direction. ρ denotes the density, c_p is the specific heat for moist air at constant pressure ($c_p = c_{pd}\,[1 + (c_{pv}/c_{pd} - 1)\,q]$, where c_{pd} and c_{pv} are the specific heats at constant pressure for dry air and water vapor, respectively). C_m is the drag coefficient, C_h is the transfer coefficient for heat, T_S is the surface temperature, q_S is the surface specific humidity and $|\vec{v}|$ is the absolute value of the horizontal velocity at the lowermost level with a prescribed minimum (default= 1 m/s) to avoid numerical problems. The wetness factor C_w accounts for different evaporation efficiencies due to surface characteristics (Section 3.5.2). u, v, T and q are the zonal and meridional wind components, the temperature and the specific humidity, respectively, of the lowermost model level. The factors γ and δ are used to relate the model quantities to the respective near surface values. δ is set to 1 and γ is set to give a potential temperature:

$$\gamma = \left(\frac{p_S}{p}\right)^{\frac{R_d}{c_{pd}}} \tag{3.2}$$

where p is the pressure of the lowermost model level, p_S is the surface pressure and R_d is the gas constant for dry air.

While γ, ρ, C_m, C_h, $|\vec{v}|$, T_S and q_S apply to time level $t - \Delta t$, values for $u^{t+\Delta t}$, $v^{t+\Delta t}$, $T^{t+\Delta t}$

and $q^{t+\Delta t}$ are computed implicitly from the discretized tendency equations:

$$\begin{aligned}
\frac{u^{t+\Delta t} - u^{t-\Delta t}}{2\Delta t} &= -\frac{1}{\rho\,\Delta z}\,F_u^{t+\Delta t} &&= -\frac{g\,\rho\,C_m\,|\vec{v}|}{p_S\,\Delta\sigma}\,u^{t+\Delta t} \\
\frac{v^{t+\Delta t} - v^{t-\Delta t}}{2\Delta t} &= -\frac{1}{\rho\,\Delta z}\,F_v^{t+\Delta t} &&= -\frac{g\,\rho\,C_m\,|\vec{v}|}{p_S\,\Delta\sigma}\,v^{t+\Delta t} \\
\frac{T^{t+\Delta t} - T^{t-\Delta t}}{2\Delta t} &= -\frac{1}{c_p\,\rho\,\Delta z}\,F_T^{t+\Delta t} &&= -\frac{g\,\rho\,C_h\,|\vec{v}|}{p_S\,\Delta\sigma}\,(\gamma T^{t+\Delta t} - T_S) \\
\frac{q^{t+\Delta t} - q^{t-\Delta t}}{2\Delta t} &= -\frac{1}{\rho\,\Delta z}\,F_q^{t+\Delta t} &&= -\frac{g\,\rho\,C_h\,C_w\,|\vec{v}|}{p_S\,\Delta\sigma}\,(\delta q^{t+\Delta t} - q_S)
\end{aligned} \tag{3.3}$$

where g is the gravitational acceleration and $\Delta\sigma = \Delta p/p_S$ is the thickness of the lowermost model layer.

In addition to the tendencies, the surface fluxes of momentum, sensible and latent heat and the partial derivative of the sensible and the latent heat flux with respect to the surface temperature are computed:

$$\begin{aligned}
F_u &= \rho\,C_m\,|\vec{v}|\,u^{t+\Delta t} \\
F_v &= \rho\,C_m\,|\vec{v}|\,v^{t+\Delta t} \\
F_T &= c_p\,\rho\,C_h\,|\vec{v}|\,(\gamma T^{t+\Delta t} - T_S) \\
L\,F_q &= L\,\rho\,C_h\,C_w\,|\vec{v}|\,(\delta q^{t+\Delta t} - q_S) \\
\frac{\partial F_T}{\partial T_S} &= -c_p\,\rho\,C_h\,|\vec{v}| \\
\frac{\partial (L\,F_q)}{\partial T_S} &= -L\,\rho\,C_h\,C_w\,|\vec{v}|\,\frac{\partial q_S(T_S)}{\partial T_S}
\end{aligned} \tag{3.4}$$

The derivatives of the fluxes may be used, for examples, for an implicit calculation of the surface temperature (see Section 3.5.1).

Drag and transfer coefficients

The calculation of the drag and the transfer coefficient C_m and C_h follows the method described in Roeckner et al. (1992) for the ECHAM-3 model, which bases on the work of Louis (1979) and Louis et al. (1982). A Richardson number dependence of C_m and C_h in accordance to the Monin-Obukhov similarity theory is given by

$$\begin{aligned}
C_m &= \left(\tfrac{k}{\ln(z/z_0)}\right)^2 f_m(Ri, z/z_0) \\
C_h &= \left(\tfrac{k}{\ln(z/z_0)}\right)^2 f_h(Ri, z/z_0)
\end{aligned} \tag{3.5}$$

where k is the von Karman constant ($k = 0.4$) and z_0 is the roughness length, which depends on the surface characteristics (Section 3.5.4 and Section 3.6). The Richardson number Ri is

defined as

$$Ri = \frac{g\,\Delta z\,(\gamma_E T - \gamma_E T_S)}{\gamma_E T\,|\vec{v}|^2} \tag{3.6}$$

where γ_E transfers temperatures to virtual potential temperatures to include the effect of moisture.

$$\gamma_E = \left(1 - \left(\frac{R_v}{R_d} - 1\right) q\right) \left(\frac{p_S}{p}\right)^{\frac{R_d}{c_{pd}}} \tag{3.7}$$

where q refers to the respective specific humidities and R_v is the gas constant for water vapor.

Different empirical formulas for stable ($Ri \geq 0$) and unstable ($Ri < 0$) situations are used. For the stable case, f_m and f_h are given by

$$\begin{aligned} f_m &= \frac{1}{1 + (2\,b\,Ri)/\sqrt{1 + d\,Ri}} \\ f_h &= \frac{1}{1 + (3\,b\,Ri)/\sqrt{1 + d\,Ri}} \end{aligned} \tag{3.8}$$

while for the unstable case, f_m and f_h are

$$\begin{aligned} f_m &= 1 - \frac{2\,b\,Ri}{1 + 3\,b\,c\,[\frac{k}{\ln(z/z_0+1)}]^2 \sqrt{-Ri\,(z/z_0+1)}} \\ f_h &= 1 - \frac{3\,b\,Ri}{1 + 3\,b\,c\,[\frac{k}{\ln(z/z_0+1)}]^2 \sqrt{-Ri\,(z/z_0+1)}} \end{aligned} \tag{3.9}$$

where b, c, and d are prescribed constants and set to default values of $b = 5$, $c = 5$ and $d = 5$.

As in ECHAM-3 for unstable condition over oceans the empirical formula from Miller et al. (1992) is used to compute C_h

$$C_h = C_{mn} \cdot (1 - C_R^{\delta})^{1/\delta} \tag{3.10}$$

with

$$C_R = \frac{0.0016 \cdot (\Delta\Theta_v)^{1/3}}{C_{mn} \cdot |\vec{v}|} \tag{3.11}$$

and

$$C_{mn} = \left(\frac{k}{\ln(z/z_0)}\right)^2 \tag{3.12}$$

δ is set to 1.25.

3.1.2 Vertical Diffusion

Vertical diffusion representing the non resolved turbulent exchange is applied to the horizontal wind components u and v, the potential temperature θ ($= T(p_S/p)^{R_d/c_{pd}}$) and the specific

humidity q. The tendencies due to the turbulent transports are given by

$$\begin{aligned}
\frac{\partial u}{\partial t} &= \frac{1}{\rho}\frac{\partial J_u}{\partial z} &= \frac{1}{\rho}\frac{\partial}{\partial z}(\rho\, K_m \frac{\partial u}{\partial z}) \\
\frac{\partial v}{\partial t} &= \frac{1}{\rho}\frac{\partial J_v}{\partial z} &= \frac{1}{\rho}\frac{\partial}{\partial z}(\rho\, K_m \frac{\partial v}{\partial z}) \\
\frac{\partial T}{\partial t} &= \frac{1}{\rho}\frac{\partial J_T}{\partial z} &= \frac{1}{\rho}\frac{\partial}{\partial z}(\rho\, K_h (\frac{p}{p_S})^{R_d/c_{pd}} \frac{\partial \theta}{\partial z}) \\
\frac{\partial q}{\partial t} &= \frac{1}{\rho}\frac{\partial J_q}{\partial z} &= \frac{1}{\rho}\frac{\partial}{\partial z}(\rho\, K_h \frac{\partial q}{\partial z})
\end{aligned} \tag{3.13}$$

where p is the pressure, p_S is the surface pressure, R_d is the gas constant for dry air and c_{pd} is the specific heat for dry air at constant pressure. Here, the turbulent fluxes (positive downward) of zonal and meridional momentum J_u and J_v, heat $c_{pd}\, J_T$ and moisture J_q are parameterized by a linear diffusion along the vertical gradient with the exchange coefficients K_m and K_h for momentum and heat, respectively. K_m and K_h depend on the actual state (see below). As the effect of the surface fluxes are computed separately (Section 3.1.1), no flux boundary conditions for the vertical diffusion scheme are assumed at the top and the bottom of the atmosphere but the vertical diffusion is computed starting with initial values for u, v, q and T which include the tendencies due to the surface fluxes.

As for the surface fluxes, the equations are formulated implicitely with exchange coefficients applying to the old time level. This leads to sets of linear equations for $u^{t+\Delta t}$, $v^{t+\Delta t}$, $T^{t+\Delta t}$ and $q^{t+\Delta t}$, which are solved by a back substitution method.

Exchange coefficients

The calculation of the exchange coefficient K_m and K_h follows the mixing length approach as an extension of the similarity theory used to define the drag and transfere coefficients (Section 3.1.1 and Roeckner et al. 1992):

$$\begin{aligned}
K_m &= l_m^2 \left|\frac{\partial \vec{v}}{\partial z}\right| f_m(Ri) \\
K_h &= l_h^2 \left|\frac{\partial \vec{v}}{\partial z}\right| f_h(Ri)
\end{aligned} \tag{3.14}$$

where the functional dependencies of f_m and f_h on Ri are the same as for C_m and C_h (Eq. 3.8 and Eq. 3.9), except that the term

$$\left[\frac{k}{\ln(z/z_0+1)}\right]^2 \sqrt{(z/z_0+1)} \tag{3.15}$$

is replaced by

$$\frac{l^2}{(\Delta z)^{3/2}\, z^{1/2}} \left[\left(\frac{z+\Delta z}{z}\right)^{1/3} - 1\right]^{3/2} \tag{3.16}$$

The Richardson number Ri is defined as

$$Ri = \frac{g}{\gamma T}\frac{\partial(\gamma_E T)}{\partial z}\left|\frac{\partial \vec{v}}{\partial z}\right|^{-2} \tag{3.17}$$

with γ from Eq. 3.2 and γ_E from Eq. 3.7. According to Blackadar (1962), the mixing lengths l_m and l_h are given by

$$\begin{aligned} \frac{1}{l_m} &= \frac{1}{k\,z} + \frac{1}{\lambda_m} \\ \frac{1}{l_h} &= \frac{1}{k\,z} + \frac{1}{\lambda_h} \end{aligned} \tag{3.18}$$

with $\lambda_h = \lambda_m \sqrt{(3d)/2}$. The parameters λ_m and d are set to default values of $\lambda_m = 160\ m$ and $d = 5$.

3.2 Horizontal Diffusion

The horizontal diffusion parameterization based on the ideas of Laursen and Eliasen (1989), which, in the ECHAM-3 model (Roeckner et al. 1992), improves the results compared with a ∇^k horizontal diffusion. The diffusion is done in spectral space. The contribution to the tendency of a spectral prognostic variable X_n is

$$\frac{\partial X_n}{\partial t} = -k_X L_n X_n \tag{3.19}$$

where n defines the total wave number. L_n is a scale selective function of the total wave number and is chosen such that large scales are not damped while the damping gets stronger with increasing n:

$$L_n = \begin{cases} (n - n_\star)^\alpha & \text{for} \quad n > n_\star \\ \\ 0 & \text{for} \quad n \leq n_\star \end{cases} \tag{3.20}$$

where $n_\star$ is a cut-off wave number. For T21 resolution the parameters $n_\star$ and α are set to default values of $n_\star = 15$ and $\alpha = 2$ similar to the ECHAM-3 model (Roeckner et al. 1992). The diffusion coefficient k_X defines the timescale of the damping and depends on the variable. In the model, k_X is computed from prescribed damping time scales τ_X for the smallest waves. Default values of $\tau_D = 0.2$ days for divergence, $\tau_\xi = 1.1$ days for vorticity and $\tau_T = 15.6$ days for temperature and $\tau_q = 0.1$ days for humidity are chosen, which are comparable with the respective values in the T21 ECHAM-3 model exept for humidity where here a considerable smaller value is used. In contrast to ECHAM-3 no level or velocity dependent additional damping is applied.

For T42 resolution the respective defaults are: $n_\star = 16$, $\alpha = 4$, $\tau_D = 0.06$ days, $\tau_\xi = 0.3$ days, $\tau_T = 0.76$ days and $\tau_q = 0.1$ days.

3.3 Radiation

3.3.1 Short Wave Radiation

The short wave radiation scheme bases on the ideas of Lacis and Hansen (1974) for the cloud free atmosphere. For the cloudy part, either constant albedos and transmissivities for high-middle- and low-level clouds may be prescribed or parameterizations following Stephens (1978) and Stephens et al. (1984) may be used.

The downward radiation flux density $F^{\downarrow SW}$ is assumed to be the product of the extraterristical solar flux density E_0 with different transmission factors for various processes:

$$F^{\downarrow SW} = \mu_0 \, E_0 \cdot \mathcal{T}_R \cdot \mathcal{T}_O \cdot \mathcal{T}_W \cdot \mathcal{T}_D \cdot \mathcal{T}_C \cdot \mathcal{R}_S \tag{3.21}$$

Here, μ_0 refers to the cosine of the solar zenith angle and the factor $\mathcal{R}_S$ incorporates different surface albedo values. The Indices of the transmissivities $\mathcal{T}$ denote Rayleigh scattering (R), ozone absorption (O), water vapor absorption (W) and absorption and scattering by aerosols (dust; D) and cloud droplets (C), respectively. E_0 and μ_0 are computed following Berger (1978a, 1978b). The algorithm used is valid to 1,000,000 years past or hence. The numeric to compute E_0 and μ_0 is adopted from the CCM3 climate model (Kiehl et al. 1996, coding by E. Kluzek 1997). The calculation accounts for earths orbital parameters and the earths distance to the sun, both depending on the year and the time of the year. In default mode the model runs with daily averaged insolation but a diurnal cycle can be switched on.

Following, for example, Stephens (1984) the solar spectral range is divided into two regions: (1) A visible and ultraviolet part for wavelengths $\lambda < 0.75$ μm with pure cloud scattering, ozone absorption and Rayleigh scattering, and without water vapor absorption. (2) A near infrared part for wavelengths $\lambda > 0.75$ μm with cloud scattering and absorption and with water vapor absorption. Absorption and scattering by aerosols is neglected in the present scheme. Dividing the total solar energy E_0 into the two spectral regions results in the fractions $E_1 = 0.517$ and $E_2 = 0.483$ for spectral ranges 1 and 2, respectively.

Clear sky

For the clear sky part of the atmospheric column parameterizations following Lacis and Hansen (1974) are used for Rayleigh scattering, ozone absorption and water vapor absorption.

Visible and ultraviolet spectral range ($\lambda < 0.75$ μm)

In the visible and ultraviolet range, Rayleigh scattering and ozone absorption are considered for the clear sky part. Rayleigh scattering is confined to the lowermost atmospheric layer. The transmissivity for this layer is given by

$$\mathcal{T}_{R1} = 1 - \frac{0.219}{1 + 0.816\mu_0} \tag{3.22}$$

for the direct beam, and

$$\mathcal{T}_{R1} = 1 - 0.144 \tag{3.23}$$

for the scattered part.

Ozone absorption is considered for the Chappuis band in the visible $\mathcal{A}^{vis}$ and for the ultraviolet range $\mathcal{A}^{uv}$. The total transmissivity due to ozone is given by

$$\mathcal{T}_{O1} = 1 - \mathcal{A}_O^{vis} - \mathcal{A}_O^{uv} \tag{3.24}$$

with

$$\mathcal{A}_O^{vis} = \frac{0.02118x}{1 + 0.042x + 0.000323x^2} \tag{3.25}$$

and

$$\mathcal{A}_O^{uv} = \frac{1.082x}{(1 + 138.6x)^{0.805}} + \frac{0.0658x}{1 + (103.6x)^3} \tag{3.26}$$

where the ozone amount traversed by the direct solar beam, x, is

$$x = M\ u_{O_3} \tag{3.27}$$

with u_{O_3} being the ozone amount [cm] in the vertical column above the considered layer, and M is the magnification factor after Rodgers (1967)

$$M = \frac{35}{(1224{\mu_0}^2 + 1)^{\frac{1}{2}}} \tag{3.28}$$

The ozone path traversed by diffuse radiation from below is

$$x^* = M\ u_{O_3} + \overline{M}\ (u_t - u_{O_3}) \tag{3.29}$$

where u_t is the total ozone amount above the main reflecting layer and $\overline{M}$=1.9 is the effective magnification factor for diffusive upward radiation.

Near infrared ($\lambda > 0.75\ \mu$m)

In the near infrared solar region absorption by water vapor is considered only. The transmissivity is given by

$$\mathcal{T}_{W2} = 1 - \frac{2.9y}{(1 + 141.5y)^{0.635} + 5.925y} \tag{3.30}$$

where y is the effective water vapor amount [cm] including an approximate correction for the pressure and temperature dependence of the absorption and the magnification factor M. For the direct solar beam, y is given by

$$y = \frac{M}{g} \int_0^p 0.1\ q \left(\frac{p}{p_0}\right) \left(\frac{T_0}{T}\right)^{\frac{1}{2}} dp \tag{3.31}$$

while for the reflected radiation reaching the layer from below, y is

$$y = \frac{M}{g} \int_0^{p_S} 0.1\ q \left(\frac{p}{p_0}\right) \left(\frac{T_0}{T}\right)^{\frac{1}{2}} dp + \frac{\beta_d}{g} \int_p^{p_S} 0.1\ q \left(\frac{p}{p_0}\right) \left(\frac{T_0}{T}\right)^{\frac{1}{2}} dp \tag{3.32}$$

with the acceleration of gravity g, the surface pressure p_S, a reference pressure $p_0 = 1000$ hPa, a reference temperature $T_0 = 273$ K, the specific humidity q [kg/kg] and the magnification factor for diffuse radiation $\beta_d = 1.66$.

Clouds

Two possibilities for the parameterization of the effect of clouds on the short wave radiative fluxes are implemented: (1) prescribed cloud properties and (2) a parameterization following Stephens (1978) and Stephens et al. (1984), which is the default setup.

Prescribed cloud properties

Radiative properties of clouds are prescribed depending on the cloud level. Albedos $\mathcal{R}_{C1}$ for cloud scattering in the visible spectral range ($\lambda < 0.75$ μm), and albedos $\mathcal{R}_{C2}$ for cloud scattering and absorptivities $\mathcal{A}_{C2}$ for cloud absorption in the near infrared part ($\lambda > 0.75$ μm) are defined for high, middle and low level clouds. The default values are listed in Table 3.1.

Cloud Level	Visible range $\mathcal{R}_{C1}$	Near infrared $\mathcal{R}_{C2}$	Near infrared $\mathcal{A}_{C1}$
High	0.15	0.15	0.05
Middle	0.30	0.30	0.10
Low	0.60	0.60	0.20

Table 3.1: Prescribed cloud albedos $\mathcal{R}_C$ and absorptivities $\mathcal{A}_C$ for spectral range 1 and 2

Default: Parameterization according to Stephens (1978) and Stephens et al. (1984)

Following Stephens (1978) and Stephens et al. (1984) cloud parameters are derived from the cloud liquid water path W_L [g/m^2] and the cosine of the solar zenith angel μ_0. In the visible and ultraviolet range cloud scattering is present only while in the near infrared both, cloud scattering and absorption, are parameterized.

Visible and ultraviolet spectral range ($\lambda < 0.75$ μm)

For the cloud transmissivity $\mathcal{T}_{C1}$ Stephens parameterization for a non absorbing medium is applied:

$$\mathcal{T}_{C1} = 1 - \frac{\beta_1 \tau_{N1}/\mu_0}{1 + \beta_1 \tau_{N1}/\mu_0} = \frac{1}{1 + \beta_1 \tau_{N1}/\mu_0} \tag{3.33}$$

β_1 is the backscatter coefficient, which is available in tabular form. In order to avoid interpolation of tabular values the following interpolation formula is used

$$\beta_1 = f_{b1} \sqrt{\mu_0} \tag{3.34}$$

where the factor f_{b1} comprises a tuning opportunity for the cloud albedo and is set to a default value of 0.0641 for T21L10 (0.02 T21L5 and 0.085 T42L10).

τ_{N1} is an effective optical depth for which Stephens (1979) provided the interpolation formula

$$\tau_{N1} = 1.8336 \, (\log W_L)^{3.963} \tag{3.35}$$

which is approximated by

$$\tau_{N1} = 2 \, (\log W_L)^{3.9} \tag{3.36}$$

to be used also for the near infrared range (see below).

Near infrared ($\lambda > 0.75$ μm)

The transmissivity due to scattering and absorption of a cloud layer in the near infrared spectral range is

$$\mathcal{T}_{C2} = \frac{4u}{R} \tag{3.37}$$

where u is given by

$$u^2 = \frac{(1 - \tilde{\omega}_0 + 2 \, \beta_2 \, \tilde{\omega}_0)}{(1 - \tilde{\omega}_0)} \tag{3.38}$$

and R by

$$R = (u+1)^2 \exp(\tau_{eff}) - (u-1)^2 \exp(-\tau_{eff}) \tag{3.39}$$

with

$$\tau_{eff} = \frac{\tau_{N2}}{\mu_0} \sqrt{(1-\tilde{\omega}_0)(1-\tilde{\omega}_0 + 2\,\beta_2\,\tilde{\omega}_0)} \tag{3.40}$$

where the original formulation for the optical depth τ_{N2} by Stephens (1978)

$$\tau_{N2} = 2.2346\,(\log W_L)^{3.8034} \tag{3.41}$$

is, as for the visible range, approximated by

$$\tau_{N2} = 2\,(\log W_L)^{3.9} \tag{3.42}$$

Approximations for the table values of the back scattering coefficient β_2 and the single scattering albedo $\tilde{\omega}_0$ are

$$\beta_2 = \frac{f_{b2}\,\sqrt{\mu_0}}{\ln(3 + 0.1\,\tau_{N2})} \tag{3.43}$$

and

$$\tilde{\omega}_0 = 1 - f_{o2}\,\mu_0^2\,\ln(1000/\tau_{N2}) \tag{3.44}$$

where f_{b2} and f_{o2} provide a tuning of the cloud properties and are set to default values of f_{b2}=0.045 and f_{o2}=0.0045 for T21L10 (0.004 T21L5, 0.0048 T42L10).

The scattered flux is computed from the cloud albedo $\mathcal{R}_{C2}$ which is given by

$$\mathcal{R}_{C2} = [\exp(\tau_{eff}) - \exp(-\tau_{eff})]\,\frac{u^2-1}{R} \tag{3.45}$$

Vertical integration

For the vertical integration, the adding method is used (e.g. Lacis and Hansen 1974, Stephens 1984). The adding method calculates the reflection $\mathcal{R}_{ab}$ and transmission $\mathcal{T}_{ab}$ functions for a composite layer formed by combining two layers one (layer a) on top of the other (layer b). For the downward beam $\mathcal{R}_{ab}$ and $\mathcal{T}_{ab}$ are given by

$$\begin{aligned} \mathcal{R}_{ab} &= \mathcal{R}_a + \mathcal{T}_a \mathcal{R}_b \mathcal{T}_a^* / (1 - \mathcal{R}_a^* \mathcal{R}_b) \\ \mathcal{T}_{ab} &= \mathcal{T}_a \mathcal{T}_b / (1 - \mathcal{R}_a^* \mathcal{R}_b) \end{aligned} \tag{3.46}$$

where the denominator accounts for multiple reflections between the two layers. For illumination form below $\mathcal{R}_{ab}^*$ and $\mathcal{T}_{ab}^*$ are given by

$$\begin{aligned} \mathcal{R}_{ab}^* &= \mathcal{R}_b^* + \mathcal{T}_b^* \mathcal{R}_a^* \mathcal{T}_b / (1 - \mathcal{R}_a^* \mathcal{R}_b) \\ \mathcal{T}_{ab}^* &= \mathcal{T}_a^* \mathcal{T}_b / (1 - \mathcal{R}_a^* \mathcal{R}_b) \end{aligned} \tag{3.47}$$

The following four steps are carried out to obtain the radiative upward and downward fluxes at the boundary between two layers from which the total flux and the absorption (heating rates) are calculated:

1) $\mathcal{R}_l$ and $\mathcal{T}_l$, $l = 1, L$ are computed for each layer and both spectral regions according to the parameterizations.

2) The layers are added, going down, to obtain $\mathcal{R}_{1,l}$ and $\mathcal{T}_{1,l}$ for $L = 2, L+1$ and $\mathcal{R}^*_{1,l}$ and $\mathcal{T}^*_{1,l}$ for $L = 2, L$.

3) Layers are added one at the time, going up, to obtain $\mathcal{R}_{L+1-l,L+1}$, $l = 1, L-1$ starting with the ground layer, $\mathcal{R}_{L+1} = \mathcal{R}_S$ which is the surface albedo and $\mathcal{T}_{L+1}$=0.

4) The upward $F_l^{\uparrow SW}$ and downward $F_l^{\downarrow SW}$ short wave radiative fluxes at the interface of layer $(1, l)$ and layer (l+1,L+1) are determined from

$$\begin{aligned} F_l^{\uparrow SW} &= \mathcal{T}_{1,l}\, \mathcal{R}_{l+1,L+1}/(1 - \mathcal{R}^*_{1,l}\, \mathcal{R}_{l+1,L+1}) \\ F_l^{\downarrow SW} &= \mathcal{T}_{1,l}/(1 - \mathcal{R}^*_{1,l}\, \mathcal{R}_{l+1,L+1}) \end{aligned} \tag{3.48}$$

The net downward flux at level l, $F_l^{\updownarrow SW}$, is given by

$$F_l^{\updownarrow SW} = F_l^{\downarrow SW} - F_l^{\uparrow SW} \tag{3.49}$$

Finally, the temperature tendency for the layer between l and $l+1$ is computed:

$$\frac{\Delta T_{l+\frac{1}{2}}}{2\Delta t} = -\frac{g}{c_p\, p_S} \frac{F_{l+1}^{\updownarrow SW} - F_l^{\updownarrow SW}}{\Delta\sigma} \tag{3.50}$$

3.3.2 Long Wave Radiation

Clear sky

For the clear sky long wave radiation, the broad band emissivity method is employed (see, for example, Manabe and Möller 1961, Rodgers 1967, Sasamori 1968, Katayama 1972, Boer et al. 1984). Using the broad band transmissivities $\mathcal{T}_{(z,z')}$ between level z and level z', the upward and downward fluxes at level z, $F^{\uparrow LW}(z)$ and $F^{\downarrow LW}(z)$, are

$$\begin{aligned} F^{\uparrow LW}(z) &= \mathcal{A}_S\, B(T_S)\mathcal{T}_{(z,0)} + \int_0^z B(T')\frac{\partial \mathcal{T}_{(z,z')}}{\partial z'}dz' \\ F^{\downarrow LW}(z) &= \int_\infty^z B(T')\frac{\partial \mathcal{T}_{(z,z')}}{\partial z'}dz' \end{aligned} \tag{3.51}$$

where $B(T)$ denotes the black body flux ($B(T) = \sigma_{SB}T^4$) and $\mathcal{A}_S$ is the surface emissivity. The effect of water vapor, carbon dioxide and ozone is included in the calculations of the transmissivities $\mathcal{T}$ (with $\mathcal{T} = 1 - \mathcal{A}$, where $\mathcal{A}$ is the absoroptivity/emissivity). The transmissivities for water vapor $\mathcal{T}_{H_2O}$, carbon dioxide $\mathcal{T}_{CO_2}$ and ozone $\mathcal{T}_{O_3}$ are taken from Sasamori (1968):

$$\mathcal{T}_{H_2O} = 1 - 0.846\,(u_{H_2O} + 3.59\cdot 10^{-5})^{0.243} - 6.90\cdot 10^{-2}$$

for $u_{H_2O} < 0.01$ g, and

$$\mathcal{T}_{H_2O} = 1 - 0.240\log(u_{H_2O} + 0.010) + 0.622$$

else.

$$\mathcal{T}_{CO_2} = 1 - 0.0825\, u_{CO_2}^{0.456} \tag{3.52}$$

for $u_{CO_2} \le 0.5$ cm, and

$$\mathcal{T}_{CO_2} = 1 - 0.0461\log(u_{CO_2}) + 0.074$$

else.

$$\mathcal{T}_{O_3} = 1 - 0.0122\log(u_{O_3} + 6.5\cdot 10^{-4}) + 0.0385$$

where u_{H_2O}, u_{CO_2} and u_{O_3} are the effective amounts of water vapor, carbon dioxide and ozone, respectively, which are obtained from:

$$u(p,p') = \frac{f}{g}\int_p^{p'} q_X\left(\frac{p''}{p_0}\right)dp'' \tag{3.53}$$

where q_X denotes the mixing ratios [kg/kg] of water vapor, carbon dioxide and ozone, respectively, g is the gravitational acceleration, p is pressure and $p_0 = 1000$ hPa is the reference pressure. The factor f is used to transfer the units to g/cm^2 for u_{H_2O} and cm-STP for u_{CO_2} and cm-STP for u_{O_3}, which are used in Eq. 3.52.

To account for the overlap between the water vapor and the carbon dioxide bands near 15 μm, the CO_2 absorption is corrected by a H_2O transmission at 15 μm, $\mathcal{T}_{H_2O}^{15\mu m}$, with $\mathcal{T}_{H_2O}^{15\mu m}$ given by

$$\mathcal{T}_{H_2O}^{15\mu m} = 1.33 - 0.832\,(u_{H_2O} + 0.0286)^{0.26} \tag{3.54}$$

Water vapour continuum absorption is parameterized by

$$\mathcal{T}_{H_2O}^{cont} = 1. - \exp(-k_{cont} u_{H_2O}) \tag{3.55}$$

with a constant k_{cont} (default =0.03 for T21L10, 0.035 T21L5,T42L10)

Clouds

Clouds can be either treated as gray bodies with a prescribed cloud flux emissivity (grayness) or the cloud flux emissivity is obtained from the cloud liquid water contend. If the cloud flux emissivity (grayness) $\mathcal{A}^{cl}$ is externally prescribed, the value is attributed to each cloud layer. Otherwise, which is the default, $\mathcal{A}^{cl}$ is calculated from the cloud liquid water (e.g. Stephens 1984)

$$\mathcal{A}^{cl} = 1. - \exp\left(-\beta_d\, k^{cl}\, W_L\right) \tag{3.56}$$

where $\beta_d = 1.66$ is the diffusivity factor, k^{cl} is the mass absorption coefficent (with is set to a default value of 0.1 m^2/g (Slingo and Slingo 1991)) and W_L is the cloud liquid water path.

For a single layer between z and z' with fractional cloud cover cc, the total transmissivity $\mathcal{T}^*_{(z,z')}$ is given by

$$\mathcal{T}^*_{(z,z')} = \mathcal{T}_{(z,z')}\,(1 - cc\,\mathcal{A}^{cl}) \tag{3.57}$$

where $\mathcal{T}_{(z,z')}$ is the clear sky transmissivity. When there is more than one cloud layer with fractional cover, random overlapping of the clouds is assumed and $\mathcal{T}^*_{(z,z')}$ becomes

$$\mathcal{T}^*_{(z,z')} = \mathcal{T}_{(z,z')} \prod_j (1 - cc_j\,\mathcal{A}^{cl}_j) \tag{3.58}$$

where the subscript j denotes the cloud layers.

Vertical discretization

To compute the temperature tendency for a model layer resulting form the divergence of the radiative fluxes, the vertical discretization scheme of Chou et al. (2002) is used. The upward and downward fluxes, $F_l^{\uparrow LW}$ and $F_l^{\downarrow LW}$, at level l, which is the interface between two model layers, are computed from

$$\begin{aligned} F_l^{\uparrow LW} &= \sum_{l'=l}^{L} B_{l'+\frac{1}{2}}[\mathcal{T}^*_{(l,l')} - \mathcal{T}^*_{(l'+1,l)}] \qquad l = 1, \cdots, L \\ &\quad + \mathcal{T}^*_{(l,L+1)}\; F_{L+1}^{\uparrow LW} \end{aligned} \tag{3.59}$$

$$F_l^{\downarrow LW} = \sum_{l'=1}^{l-1} B_{l'+\frac{1}{2}}[\mathcal{T}^*_{(l'+1,l)} - \mathcal{T}^*_{(l',l)}] \qquad l = 2, \cdots, L+1$$

where $\mathcal{T}^*_{(l,l')}$ denotes the transmissivity of the layer from level l to level l' (see above) and $B_{l+\frac{1}{2}}$ is the black body flux for level $l+\frac{1}{2}$. The downward flux at the top of the atmosphere, $F_0^{\downarrow LW}$, and the upward flux at the surface ,$F_{L+1}^{\uparrow LW}$, are given by

$$\begin{aligned} F_0^{\downarrow LW} &= 0 \\ F_{L+1}^{\uparrow LW} &= \mathcal{A}_S\, B(T_S) + (1-\mathcal{A}_S)\, F_{L+1}^{\downarrow LW} \end{aligned} \tag{3.60}$$

where $\mathcal{A}_S$ denotes the surface emissivity and T_S is the surface temperature. Note, that for a more convenient discription of the scheme, $l+\frac{1}{2}$ denotes a so called full level, where the temperatures are defined. This may be in contrast to the convention in most of the other sections where a full level is indicated by l.

Eqs. 3.59 can be rearranged to give

$$\begin{aligned} F_l^{\uparrow LW} &= B_{l+\frac{1}{2}} + \sum_{l'=l+1}^{L+1} \mathcal{T}^*_{(l',l)} \left[B_{l'+\frac{1}{2}} - B_{l'-\frac{1}{2}}\right] \qquad l = 1, \cdots, L \\ &\quad + \mathcal{T}^*_{(l,L+1)} \,(1-\mathcal{A}_S)\, F_{L+1}^{\downarrow LW} \end{aligned} \tag{3.61}$$

$$F_{l'}^{\downarrow LW} = B_{l'-\frac{1}{2}} - \sum_{l=1}^{l'-1} \mathcal{T}^*_{(l',l)} \left[B_{l+\frac{1}{2}} - B_{l-\frac{1}{2}}\right] \qquad l' = 2, \cdots, L+1$$

with the boundary conditions

$$\begin{aligned} B_{L+\frac{3}{2}} &= \mathcal{A}_S\, B(T_S) \\ B_{\frac{1}{2}} &= 0 \end{aligned} \tag{3.62}$$

The net downward flux at level l, $F_l^{\updownarrow LW}$, is given by

$$F_l^{\updownarrow LW} = F_l^{\downarrow LW} - F_l^{\uparrow LW} \tag{3.63}$$

Finally, the temperature tendency for the layer between l and $l+1$ is computed:

$$\frac{\Delta T_{l+\frac{1}{2}}}{2\Delta t} = -\frac{g}{c_p\, p_S} \frac{F_{l+1}^{\updownarrow LW} - F_l^{\updownarrow LW}}{\Delta\sigma} \tag{3.64}$$

Emission of a layer

As pointed out by Chou et al. (2002), the difference between the upward and downward emission of a layer will be large, if the layer is rather opaque and the temperature range across the layer is large. This, in particular, holds for coarse vertical resolution as in the default version of the model. Therefore, the upward and the downward emission of a layer is computed separately following the ideas of Chou et al. (2002):

The contribution of the upward flux at level p from the adjecant layer below can be written as

$$\Delta F^{\uparrow LW}(p) = -\int_p^{p+\Delta p} B(p')\, \frac{\partial \mathcal{T}_{(p,p')}}{\partial p'}\, dp' = B^u\, (1 - \mathcal{T}_{(p+\Delta p,p)}) \tag{3.65}$$

where Δp is the thickness of the adjacent layer, B^u is the effective Planck flux for the adjacent layer, and $\mathcal{T}_{(p+\Delta p,p)}$ is the flux transmittance between p and $p+\Delta p$. Assuming that

the Planck function varies linearly with pressure and the transmittance decreases exponentially with pressure away from p it follows

$$B(p') = B(p) + \frac{(B(p) - B(p+\Delta p))(p'-p)}{\Delta p} \tag{3.66}$$

and

$$\mathcal{T}_{(p,p')} = \exp\left(-c\,(p'-p)\right) \tag{3.67}$$

with c ia a constant. From Eq. 3.65 the effective Planck flux for the adjacent layer B^u is

$$B^u = \frac{B(p) - B(p+\Delta p)\,\mathcal{T}_{(p+\Delta p,p)}}{1-\mathcal{T}_{(p+\Delta p,p)}} + \frac{B(p) - B(p+\Delta p)}{\ln(\mathcal{T}_{(p+\Delta p,p)})} \tag{3.68}$$

Similarly, for the downward flux at the lower boundary of the layer, the effective Planck function of the layer B^d is

$$B^d = \frac{B(p+\Delta p) - B(p)\,\mathcal{T}_{(p+\Delta p,p)}}{1-\mathcal{T}_{(p+\Delta p,p)}} + \frac{B(p+\Delta p) - B(p)}{\ln(\mathcal{T}_{(p+\Delta p,p)})} \tag{3.69}$$

Replacing the respective Planck functions in Eqs. 3.61 by B^u and B^d results in

$$\begin{aligned} F_l^{\uparrow LW} &= B^u_{l+\frac{1}{2}} + \sum_{l'=l+1}^{L+1} \mathcal{T}^*_{(l',l)}\,[B^u_{l'+\frac{1}{2}} - B^u_{l'-\frac{1}{2}}] \qquad l = 1,\cdots,L \\ &\quad + \mathcal{T}^*_{(l,L+1)}\,(1-\mathcal{A}_S)\,F^{\downarrow LW}_{L+1} \end{aligned} \tag{3.70}$$

$$F_{l'}^{\downarrow LW} = B^d_{l'-\frac{1}{2}} - \sum_{l=1}^{l'-1} \mathcal{T}^*_{(l',l)}\,[B^d_{l+\frac{1}{2}} - B^d_{l-\frac{1}{2}}] \qquad l' = 2,\cdots,L+1$$

where

$$\begin{aligned} B^d_{l'-\frac{1}{2}} &= \frac{B_{l'} - B_{l'-1}\,\mathcal{T}_{(l',l'-1)}}{1-\mathcal{T}_{(l',l'-1)}} + \frac{B_{l'} - B_{l'-1}}{\ln(\mathcal{T}_{(l',l'-1)})} \\ B^u_{l'-\frac{1}{2}} &= (B_{l'} + B_{l'-1}) - B^d_{l'-\frac{1}{2}} \end{aligned} \tag{3.71}$$

For the calculation of the effective Plank function, the mean transmissivity for a layer partially filled with clouds is given by

$$\mathcal{T}_{(l',l'-1)} = f_{\mathcal{T}}\,\mathcal{T}^{cs}_{(l',l'-1)}\,(1 - cc_{(l',l'-1)}\mathcal{A}^{cl}_{(l',l'-1)}) \tag{3.72}$$

with the cloud emissivity $\mathcal{A}^{cl}$ and the clear sky transmissivity $\mathcal{T}^{cs}$ being defined above, and the factor $f_{\mathcal{T}}$ provides a tuning opportunity.

When a model layer spans a region where the temperature lapse rate changes signs, the linearity of B with respect to p can not longer be assumed and B^d and B^u are simply computed from

$$B^u_{l+\frac{1}{2}} = B^d_{l-\frac{1}{2}} = 0.5\,B_{l+\frac{1}{2}} + 0.25\,(B_l + B_{l'}) \tag{3.73}$$

3.3.3 Ozone

Ozone concentration is prescribed. Either a three dimensional ozone distribution can be externally provided or an idealized annual cycle of ozone concentration can be used. The idealized distribution bases on the analytic ozone distribution of Green (1964):

$$u_{O_3}(h) = \frac{a + a\ \exp\left(-b/c\right)}{1 + \exp((h-b)/c)} \tag{3.74}$$

where $u_{O_3}(h)$ is the ozone amount [cm-STP] in a vertical column above the altitude h, a is the total ozone amount in a vertical column above the ground, b the altitude at which the ozone concentration has its maximum. While for $a = 0.4$ cm, $b = 20$ km and $c = 5$ km this distribution fits close to the mid-latitude winter ozone distribution, an annual cycle and a latitudinal dependence is introduced by varying a with time t and latitude ϕ:

$$a(t,\phi) = a0 + a1 \cdot |\sin(\phi)| + ac \cdot \sin(\phi) \cdot \cos(2\pi(d - doff)/ndy) \tag{3.75}$$

where d is the actual day of the year, $doff$ an offset and ndy the number of days per year. The defaults for the involved parameters are: $a0 = 0.25$, $a1 = 0.11$ and $ac = 0.08$.

3.3.4 Additional Newtonian cooling

For the standard setup with a vertical resolution of five equally spaced sigma-levels, the model produces a strong bias in the stratospheric (uppermost level) temperatures. This may be attributed to the insufficient representation of the stratosphere and its radiative and dynamical processes. The bias also effects the tropospheric circulation leading, for example, to a misplacement of the dominant pressure centers. To enable the simulation of a more realistic tropospheric climate, a Newtonian cooling can be applied to the uppermost level. Using this method, the model temperature T is relaxed towards a externally given distribution of the temperature T_{NC} which results in additional temperature tendencies $\dot{T}$ for the uppermost model level of

$$\dot{T} = \frac{T_{NC} - T}{\tau_{NC}} \tag{3.76}$$

where τ_{NC} is the time scale of the relaxation, which has a default value of ten days.

3.4 Moist Processes and Dry Convection

3.4.1 Correction of Negative Humidity

Local negative values of specific humidity are an artifact of spectral models. In the model, a simple procedure corrects these negative values by conserving the global amount of water. The correction of negative moisture is performed at the beginning of the grid-point parameterization scheme. A negative value of specific humidity is reset to zero. Accumulation of all corrections defines a correction factor. A hierarchical scheme of three steps is used. First, the correction is done within an atmospheric column only. If there are atmospheric columns without sufficient moisture, a second correction step is done using all grid points of the respective latitude. Finally, if there is still negative humidity remaining, a global correction is performed.

3.4.2 Saturation Specific Humidity

For parameterizations of moist processes like cumulus convection and large scale condensation the computation of the saturation specific humidity $q_{sat}(T)$ and its derivative with respect to temperature $dq_{sat}(T)/dT$ is needed at several places. In the model, the Tetens formula (Lowe 1977) is used to calculate the saturation pressure $e_{sat}(T)$ and its derivative with respect to temperature $de_{sat}(T)/dT$:

$$\begin{aligned} e_{sat}(T) &= a_1 \exp\left(a_2 \frac{T - T_0}{T - a_3}\right) \\ \frac{de_{sat}(T)}{dT} &= \frac{a_2 \,(T_0 - a_3)}{(T - a_3)^2}\, e_{sat}(T) \end{aligned} \tag{3.77}$$

with the constants $a_1 = 610.78$, $a_2 = 17.2693882$, $a_3 = 35.86$ and $T_0 = 273.16$. The saturation specific humidity $q_{sat}(T)$ and its derivative $dq_{sat}(T)/dT$ are given by

$$\begin{aligned} q_{sat}(T) &= \frac{\epsilon\, e_{sat}(T)}{p - (1 - \epsilon)\, e_{sat}(T)} \\ \frac{dq_{sat}(T)}{dT} &= \frac{p\, q_{sat}(T)}{p - (1 - \epsilon)\, e_{sat}(T)} \frac{de_{sat}(T)}{dT} \end{aligned} \tag{3.78}$$

where p is the pressure and ϵ is the ration of the gas constants for dry air R_d and water vapor R_v ($\epsilon = R_d/R_v$).

3.4.3 Cumulus Convection

The cumulus convection is parameterized by a Kuo-type convection scheme (Kuo 1965, 1974) with some modifications to the original Kuo-scheme. The Kuo-scheme considers the effect of cumulus convection on the large scale flow applying the following assumptions. Cumulus clouds are forced by mean low level convergence in regions of conditionally unstable stratification. The production of cloud air is proportional to the net amount of moisture convergence into one grid box column plus the moisture supply by surface evaporation. In a modification to the original scheme, the implemented scheme also considers clouds which originate at upper levels where moisture convergence is observed. This type of cloud may occur in mid-latitude frontal regions. Therefore, only the moisture contribution which takes place in the layer between the lifting

level and the top of the cloud is used instead of the whole column. Thus, the total moisture supply I in a period $2\Delta t$ is given by

$$I = \frac{2\Delta t\, p_S}{g} \int_{\sigma_{Top}}^{\sigma_{Lift}} A_q \, d\sigma \tag{3.79}$$

where A_q is the moisture convergence plus the surface evaporation if the lifting level σ_{Lift} is the lowermost model level. σ_{Top} is the cloud top level, p_S is the surface pressure and g is the gravitational acceleration. Lifting level, cloud base and cloud top are determined as follows. Starting form the lowermost level, the first level with positive moisture supply A_q is considered as a lifting level. If the lowermost level L is considered to be a lifting level and the surface layer is dry adiabatic unstable ($\theta_S > \theta_L$ where θ denotes the potential temperature), the convection starts from the surface. Air from the lifting level $(l+1)$ is lifted dry adiabatically up to the next level (l) by keeping its specific humidity. A cloud base is assumed to coincide with level $l + \frac{1}{2}$ if the air is saturated at l. Above the cloud base the air is lifted moist adiabatically. Distribution of temperature T_{cl} and of moisture q_{cl} in the cloud is found by first lifting the air dry adiabatically

$$\begin{aligned} (T_{cl})_l^{Ad} &= (T_{cl})_{l+1} \left(\frac{\sigma_l}{\sigma_{l+1}} \right)^{\frac{R_d}{c_{pd}}} \\ (q_{cl})_l^{Ad} &= (q_{cl})_{l+1} \end{aligned} \tag{3.80}$$

and then by correcting temperature and moisture values due to the condensation of water vapor

$$\begin{aligned} (T_{cl})_l &= (T_{cl})_l^{Ad} + \frac{L}{c_p} \frac{(q_{cl})_l^{Ad} - q_{sat}[(T_{cl})_l^{Ad}]}{1 + \frac{L}{c_p} \frac{dq_{sat}[(T_{cl})_l^{Ad}]}{dT}} \\ (q_{cl})_l &= (q_{cl})_l^{Ad} - \frac{(q_{cl})_l^{Ad} - q_{sat}[(T_{cl})_l^{Ad}]}{1 + \frac{L}{c_p} \frac{dq_{sat}[(T_{cl})_l^{Ad}]}{dT}} \end{aligned} \tag{3.81}$$

where the suturation specific humidity q_{sat} and its derivative with respect to temperature dq_{sat}/dT are computed from Eqs. 3.78. L is either the latent heat of vapourisation L_v or the latent heat of sublimation L_s depending on the temperature. c_p is the specific heat for moist air at constant pressure ($c_p = c_{pd}\,[1 + (c_{pv}/c_{pd} - 1)\,q]$ where c_{pd} and c_{pv} are the specific heats at constant pressure for dry air and water vapor, respectively) and R_d in Eq. 3.80 is the gas constant for dry air. For reasons of accuracy the calculation (3.81) is repeated once where $(T_{cl})^{Ad}$ and $(q_{cl})^{Ad}$ are now replaced by the results of the first iteration.

Cumulus clouds are assumed to exist only if the environmental air with temperature T_e and moisture q_e is unstable stratified with regard to the rising cloud parcel:

$$(T_{cl})_l > (T_e)_l \tag{3.82}$$

The top of the cloud σ_{Top} is then defined as

$$\sigma_{Top} = \sigma_{l+\frac{1}{2}} \text{ if } \begin{cases} (T_{cl})_l \leq (T_e)_l & \text{and} \\ (T_{cl})_{l+1} > (T_e)_{l+1} \end{cases} \tag{3.83}$$

Cumulus clouds do exist only if the net moisture accession I as given by Eq. 3.79 is positive. Once this final check has been done, the heating and moistening of the environmental air and the convective rain are computed.

In the model either the original scheme proposed by Kuo (1968) or the modified scheme with the parameter β (Kuo 1974) can be chosen, where β determines the partitioning of heating and moistening of the environmental air. In the scheme without β the surplus P of total energy of the cloud against the environmental air is given by

$$P = \frac{p_s}{g} \int_{\sigma_{Top}}^{\sigma_{Base}} (c_p (T_{cl} - T_e) + L (q_{sat}(T_e) - q_e)) d\sigma \tag{3.84}$$

The clouds produced dissolve instantaneously by artificial mixing with the environmental air, whereby the environment is heated and moistened by

$$\begin{aligned} (\Delta T)^{cl} &= a (T_{cl} - T_e) \\ (\Delta q)^{cl} &= a (q_{sat}(T_e) - q_e) \end{aligned} \tag{3.85}$$

where a is the fractional cloud area being produced by the moisture supply:

$$a = L \frac{I}{P} \tag{3.86}$$

In the scheme with β the fraction 1-β of the moisture is condensed, while the remaining fraction β is stored in the atmosphere. The parameter β depends on the mean relative humidity and, in the present scheme, is given by

$$\beta = \left(1 - \frac{1}{\sigma_{Base} - \sigma_{Top}} \int_{\sigma_{Top}}^{\sigma_{Base}} \frac{q_e}{q_{sat}(T_e)} d\sigma \right)^3 \tag{3.87}$$

Instead of Eq. 3.85, the temperature and moisture tendencies are now

$$\begin{aligned} (\Delta T)^{cl} &= a_T (T_{cl} - T_e) \\ (\Delta q)^{cl} &= a_q (q_{sat}(T_e) - q_e) \end{aligned} \tag{3.88}$$

where a_T and a_q are given by

$$\begin{aligned} a_T &= \frac{(1-\beta) L I}{c_p \frac{p_S}{g} \int_{\sigma_{Top}}^{\sigma_{Base}} (T_{cl} - T_e) d\sigma} \\ a_q &= \frac{\beta I}{\frac{p_S}{g} \int_{\sigma_{Top}}^{\sigma_{Base}} (q_{sat}(T_e) - q_e) d\sigma} \end{aligned} \tag{3.89}$$

The final tendencies for moisture $\partial q/\partial t$ and temperature $\partial T/\partial t$ which enter the diabatic leap frog time step are given by

$$\begin{aligned} \frac{\partial q}{\partial t} &= \frac{(\Delta q)^{cl}}{2\Delta t} - \delta^{cl} A_q \\ \frac{\partial T}{\partial t} &= \frac{(\Delta T)^{cl}}{2\Delta t} \end{aligned} \tag{3.90}$$

where δ^{cl} is specified by

$$\delta^{cl} = \begin{cases} 1 & \text{if } \sigma_{Top} \leq \sigma \leq \sigma_{Lift} \\ \\ 0 & \text{otherwise} \end{cases} \tag{3.91}$$

and $2\Delta t$ is the leap frog time step of the model. The convective precipitation rate P_c [m/s] of each cloud layer is

$$P_c = \frac{c_p\,\Delta p}{L\,g\,\rho_{H_2O}} \frac{(\Delta T)^{cl}}{2\Delta t} \tag{3.92}$$

where Δp is the pressure thickness of the layer and ρ_{H_2O} is the density of water. $(\Delta T)^{cl}$ is computed from Eq. 3.85 or Eq. 3.88, respectively.

3.4.4 Shallow Convection

In addition to deep convection a shallow convection scheme is included. Following Tiedtke (1983) shallow convection is parameterized by means of a vertical diffusion of moisture and potential temperature (and, optional, momentum). It is only applied, when the penetrative convection is not operating due to the lack of moisture or (optional) if the unstable layer is below a given threshold height(default is 700hPa). The numerical scheme is similar to that of the normal vertical diffusion (see section 3.1.2 but with a constant diffusion coefficient K which is set to default of 10 m^2/s within the cloud layer and

$$10 \cdot \frac{rh_k - 0.8}{1 - 0.8}(rh_{k+1} - rh_k) \tag{3.93}$$

at cloud top (here rh_k and rh_{k+1} denote the relative humidity at level above the cloud and the uppermost cloud level, respectively).$K = 0.$ elsewhere. The diffusion is limited to the lower part of the atmosphere up to a given pressure (set to a default of 700hPa). For the five level version, the shallow convection is switched off.

3.4.5 Large Scale Precipitation

Large scale condensation occurs if the air is supersaturated ($q > q_{sat}(T)$). Condensed water falls out instantaneously as precipitation. No storage of water in clouds is considered. An iterative procedure is used to compute final values (T^*, q^*) starting from the supersaturated state (T, q):

$$\begin{aligned} T^* &= T + \frac{L}{c_p} \frac{q - q_{sat}(T)}{1 + \frac{L}{c_p}\frac{dq_{sat}(T)}{dT}} \\ \\ q^* &= q - \frac{q - q_{sat}(T)}{1 + \frac{L}{c_p}\frac{dq_{sat}(T)}{dT}} \end{aligned} \tag{3.94}$$

where the suturation specific humidity q_{sat} and its derivative with respect to temperature dq_{sat}/dT are computed from Eqs. 3.78. L is either the latent heat of vapourisation or the latent heat of sublimation depending on the temperature. c_p is the specific heat for moist air at constant pressure ($c_p = c_{pd}\,[1 + (c_{pv}/c_{pd} - 1)\,q]$ where c_{pd} and c_{pv} are the specific heats at constant pressure for dry air and water vapor, respectively). This calculation is repeated once

using (T^*, q^*) as the new initial state. Finally, The temperature and moisture tendencies and the precipitation rate P_l [m/s] are computed:

$$\begin{aligned} \frac{\partial T}{\partial t} &= \frac{T^* - T}{2\Delta t} \\ \frac{\partial q}{\partial t} &= \frac{q^* - q}{2\Delta t} \\ P_l &= \frac{p_S \, \Delta\sigma}{g \, \rho_{H_2O}} \frac{(q - q^*)}{2\Delta t} \end{aligned} \tag{3.95}$$

where p_S is the surface pressure, ρ_{H_2O} is the density of water, $\Delta\sigma$ is the layer thickness and $2\Delta t$ is the leap frog time step of the model.

3.4.6 Cloud Formation

Cloud cover and cloud liquid water content are diagnostic quantities. The fractional cloud cover of a grid box, cc, is parameterized following the ideas of Slingo and Slingo (1991) using the relative humidity for the stratiform cloud amount cc_s and the convective precipitation rate P_c [mm/d] for the convective cloud amount cc_c. The latter is given by

$$cc_c = 0.245 + 0.125 \ln (P_c) \tag{3.96}$$

where $0.05 \leq cc_c \leq 0.8$.

Before computing the amount of stratiform clouds, the relative humidity rh is multiplied by $(1 - cc_c)$ to account for the fraction of the grid box covered by convective clouds. If $cc_c \geq 0.3$ and the cloud top is higher than $\sigma = 0.4$ ($\sigma = p/p_S$), anvil cirrus is present and the cloud amount is

$$cc_s = 2 \, (cc_c - 0.3) \tag{3.97}$$

High-, middle- and low-level stratiform cloud amounts are computed from

$$cc_s = f_\omega \left(\frac{rh - rh_c}{1 - rh_c} \right)^2 \tag{3.98}$$

where rh_c is a level depending critical relative humidity. Optionally, a restriction of low-level stratiform cloud amount due to subsidence can by introduced by the factor f_ω where f_ω is depends on the vertical velocity ω. In the default version, $f_\omega = 1$.

Cloud liquid water content q_{H_2O} [kg/kg] is computed according to Kiehl et al. (1996):

$$q_{H_2O} = \frac{q^0_{H_2O}}{\rho} \exp (-z/h_l) \tag{3.99}$$

where the reference value $q^0_{H_2O}$ is $0.21 \cdot 10^{-3}$ kg/m^3, ρ is the air density, z is the height and the local cloud water scale height h_l [m] is given by vertically integrated water vapor (precipitable water)

$$h_l = 700 \ln \left(1 + \frac{1}{g} \int_0^{p_s} q dp \right) \tag{3.100}$$

3.4.7 Evaporation of Precipitation and Snow Fall

Possible phase changes of convective or large scale precipitation within the atmosphere are considered by melting or freezing of the precipitation depending on the respective level temperature (using 273.16K as a threshold), and by evaporation parameterized in terms of the saturation deficit according to

$$E_0 = -\frac{1}{\Delta t} \cdot \frac{\gamma \cdot (q_0 - q_s)}{1 + \frac{L \cdot dq_s/dT}{C_{pd}(1+(\delta-1)q_v)}} \tag{3.101}$$

γ is set to a default of 0.01 for T21L10 (0.006 T21L5, 0.007 T42L10).

3.4.8 Dry Convective Adjustment

Dry convective adjustment is performed for layers which are dry adiabatically unstable, e.g. $\partial\theta/\partial p > 0$ where θ denotes the potential temperature. The adjustment is done so that the total sensible heat of the respective column is conserved. Wherever dry convection occurs, it is assumed that the moisture is completely mixed by the convective process as well. The adjustment is done iteratively. The atmospheric column is scanned for unstable regions. A new neutral stable state for the unstable region is computed which consists of a potential temperature θ_N and specific humidity q_N:

$$\begin{aligned} \theta_N &= \frac{\sum_{l=l_1}^{l_2} T_l \, \Delta\sigma_l}{\sum_{l=l_1}^{l_2} \sigma_l^\kappa \, \Delta\sigma_l} \\ q_N &= \frac{\sum_{l=l_1}^{l_2} q_l \, \Delta\sigma_l}{\sum_{l=l_1}^{l_2} \Delta\sigma_l} \end{aligned} \tag{3.102}$$

where l_1 and l_2 define the unstable region, $\sigma = (p/p_S)$ is the vertical coordinate, T and q are temperature and specific humidity, respectively, and κ is R_d/c_{pd} where R_d and c_{pd} are the gas constant and the specific heat for dry air, respectively.

The procedure is repeated starting from the new potential temperatures und moistures until all unstable regions are removed. The temperature and moisture tendencies which enter the diabatic time steps are then computed from the final θ_N and q_N

$$\begin{aligned} \frac{T_l^{t+\Delta t} - T_l^{t-\Delta t}}{2\Delta t} &= \frac{\theta_N \, \sigma_l^\kappa - T_l^{t-\Delta t}}{2\Delta t} \\ \frac{q_l^{t+\Delta t} - q_l^{t-\Delta t}}{2\Delta t} &= \frac{q_N - q_l^{t-\Delta t}}{2\Delta t} \end{aligned} \tag{3.103}$$

3.5 Land Surface and Soil

The parameterizations for the land surface and the soil include the calculation of temperatures for the surface and the soil, a soil hydrology and a river transport scheme. In addition, surface properties like the albedo, the roughness length or the evaporation efficiency are provided. As, at the moment, coupling to an extra glacier module is not available, glaciers are treated like other land points, but with surface and soil properties appropriate for ice. Optionally, A simple biome model can be used (simba).

3.5.1 Temperatures

The surface temperature T_S is computed from the linearized energy balance of the uppermost z_{top} meters of the ground:

$$c_{top}\ z_{top}\ \frac{\Delta T_S}{\Delta t} = F_S - G + \Delta T_S\ \frac{\partial (Q_a - F_g)}{\partial T_S} - F_m \tag{3.104}$$

z_{top} is a prescribed parameter and set to a default value of $z_{top} = 0.20$ m. Q_a denotes the total heat flux from the atmosphere, which consists of the sensible heat flux, the latent heat flux, the net short wave radiation and the net long wave radiation. Q_g is the flux into the deep soil. Q_a and Q_g are defined positive downwards. Q_m is the snow melt heat flux and c_{top} is the volumetric heat capacity. Depending on the snow pack, z_{top} can partly or totally consist of snow or soil solids: $z_{top} = z_{snow} + z_{soil}$. Thus, the heat capacity c_{top} is a combination of snow and soil heat capacities:

$$c_{top} = \frac{c_{snow}\ c_{soil}\ z_{top}}{c_{snow}\ z_{soil} + c_{soil}\ z_{snow}} \tag{3.105}$$

The default value of c_{snow} is $0.6897 \cdot 10^6$ J/(kg K) using a snow density of 330 kg/m^3. c_{soil} is set to a default value of $2.07 \cdot 10^6$ J/(kg K) for glaciers and to a value of $2.4 \cdot 10^6$ J/(kgK) otherweise.

Below z_{top} the soil column is discretized into N layers with thickness Δz_i, where layer 1 is the uppermost of the soil layers. The default values for the model are $N = 5$ and $\Delta z =$ (0.4 m, 0.8 m, 1.6 m, 3.2 m, 6.4 m). The heat flux into layer 1, Q_g, is given by

$$Q_g = \frac{2k_1}{\Delta z_1}(T_S - T_1) \tag{3.106}$$

where k_1 and T_1 are the thermal conductivity and the temperature. If the snow depth is greater than z_{top}, the thermal properties of snow are blended with the first soil layer to create a snow/soil layer with thickness $z_{snow} - z_{top} + \Delta z_1$. The thermal conductivity k_1 and heat capacity c_1 of a snow/soil layer are

$$\begin{aligned} k_1 &= \frac{k_{snow}\ k_{soil}\ (\Delta z_1 + z_{snow} - z_{top})}{k_{snow}\ \Delta z_1 + k_{soil}\ (z_{snow} - z_{top})} \\ c_1 &= \frac{c_{snow}\ c_{soil}\ (\Delta z_1 + z_{snow} - z_{top})}{c_{snow}\ \Delta z_1 + c_{soil}\ (z_{snow} - z_{top})} \end{aligned} \tag{3.107}$$

with default values of $k_{snow} = 0.31$ W/(m K), $k_{soil} = 2.03$ W/(m K) for glaciers and $k_{soil} = 7$ W/(m K) otherweise.

After the surface temperature T_S has been calculated from Eq. 3.104, snow melts when T_S is greater than the freezing temperature T_{melt}. In this case, T_S is set to T_{melt} and a new atmospheric heat flux $Q_a(T_{melt})$ is calculated from Q_a and $\partial Q_a/\partial T_S$. If the energy inbalance

is positive ($Q_a(T_{melt}) > c_{top}\ z_{top}\ (T_{melt} - T_S^t)/\Delta t$; where T_S^t is the surface temperature at the previous time step), the snow melt heat flux Q_m is

$$Q_m = \max(Q_a(T_{melt}) - \frac{c_{top}\ z_{top}}{\Delta t}\ (T_{melt} - T_S^t),\ \frac{W_{snow}\ L_f}{\Delta t}) \tag{3.108}$$

where W_{snow} is the mass of the snow water of the total snow pack and L_f is the latent heat of fusion. Any excess of energy is used to warm the soil.

With the heat flux F_z at depth z of the soil

$$F_z = -k\ \frac{\partial T}{\partial z} \tag{3.109}$$

one dimensional energy conservation requires

$$c\ \frac{\partial T}{\partial t} = -\frac{\partial F_z}{\partial z} = \frac{\partial}{\partial z}\left[k\ \frac{\partial T}{\partial z}\right] \tag{3.110}$$

where c is the volumetric soil heat capacity, T is the soil temperature, and k is the thermal conductivity.

In the model, thermal properties (temperature, thermal conductivity, volumetric heat capacity) are defined at the center of each layer. Assuming the heat flux from i to the interface i and $i+1$ equals the heat flux from the interface to $i+1$, the heat flux F_i from layer i to layer $i+1$ (positive downwards) is given by

$$F_i = -\frac{2\ k_i\ k_{i+1}(T_i - T_{i+1})}{k_{i+1}\ \Delta z_i + k_i\ \Delta z_{i+1}} \tag{3.111}$$

The energy balance for layer i is

$$\frac{c_i\ \Delta z_i}{\Delta t}\ (T_i^{t+\Delta t} - T_i^t) = F_i - F_{i-1} \tag{3.112}$$

The boundary conditions are zero flux at the bottom of the soil column and heat flux F_g at the top.

This equation is solved implicitly using fluxes F_i evaluated at $t + \Delta t$

$$\begin{aligned}
\frac{c_i \Delta z_i}{\Delta t}(T_i^{t+\Delta t} - T_i^t) &= \frac{k_i k_{i+1}(T_{i+1}^{t+\Delta t} - T_i^{t+\Delta t})}{k_{i+1}\Delta z_i + k_i \Delta z_{i+1}} + G && for \quad i = 1 \\
\frac{c_i \Delta z_i}{\Delta t}(T_i^{t+\Delta t} - T_i^t) &= \frac{k_i k_{i+1}(T_{i+1}^{t+\Delta t} - T_i^{t+\Delta t})}{k_{i+1}\Delta z_i + k_i \Delta z_{i+1}} + \frac{k_i k_{i-1}(T_{i-1}^{t+\Delta t} - T_i^{t+\Delta t})}{k_{i-1}\Delta z_i + k_i \Delta z_{i-1}} && for \quad 1 < i < N \\
\frac{c_i \Delta z_i}{\Delta t}(T_i^{t+\Delta t} - T_i^t) &= \frac{k_i k_{i-1}(T_{i-1}^{t+\Delta t} - T_i^{t+\Delta t})}{k_{i-1}\Delta z_i + k_i \Delta z_{i-1}} && for \quad i = N
\end{aligned} \tag{3.113}$$

resulting in a linear system for the $T_i^{t+\Delta t}$.

3.5.2 Soil Hydrology

The parameterization of soil hydrology comprises the budgets for snow amount and the soil water amount. The water equivalent of the snow layer $z_{snow}^{H_2O}$ is computed over land and glacier areas from

$$\frac{\partial z_{snow}^{H_2O}}{\partial t} = F_q + P_{snow} - M_{snow} \tag{3.114}$$

where F_q is the evaporation rate over snow computed from Eq. 3.4, P_{snow} is the snow fall and M_{snow} is the snow melt rate (all fluxes are positive downward and in m/s). M_{snow} is related to the snow melt heat flux Q_m (Eq. 3.108) by

$$M_{snow} = \frac{Q_m}{\rho_{H_2O}\, L_f} \tag{3.115}$$

where L_f is the latent heat of fusion.

The soil water reservoir W_{soil} [m] is represented by a single-layer bucket model (Manabe 1969). Soil water is increased by precipitation P and snow melt M_{snow} and is depleted by the surface evaporation F_q:

$$\frac{\partial W_{soil}}{\partial t} = P + M + F_q \tag{3.116}$$

where all fluxes are defined positive downwards and in m/s. Soil water is limited by a field capacity W_{max} which geographical distribution can be prescribed via an external input or is set to a default value of 0.5 m everywhere. If the soil water exceeds W_{max} the excessive water builds the runoff R and is provided to the river transport scheme (Section 3.5.3). The ratio of the soil water and the field capacity defines the wetness factor C_w which is used in Eq. 3.4 to compute the surface evaporation:

$$C_w = \frac{W_{soil}}{f_{Cw}\, W_{max}} \tag{3.117}$$

where the factor f_{Cw} (with a default value of 0.25) takes into account that maximum evaporation will take place even if the bucket is not completely filled. For land points covered by glaciers, C_w is set to a constant value of 1.

3.5.3 River Transport

The local runoff is transported to the ocean by a river transport scheme with linear advection (Sausen et al. 1994). For each grid box (both, land and ocean costal points) the river water amount W_{river} [m^3] is computed from

$$\frac{\partial W_{river}}{\partial t} = ADV + area\ (R - S) \tag{3.118}$$

where R is the local runoff (Section 3.5.2), S is the input into the ocean, ADV is the advection of river water and $area$ is the area of the respective grid box. The input into the ocean S is given by

$$S = \begin{cases} 0 & \text{for land points} \\ \\ ADV & \text{for ocean points} \end{cases} \tag{3.119}$$

This ensures that S is non-zero only for ocean costal points. The advection from grid box (i,j) into grid box (i',j'), $ADV_{(i,j)\to(i',j')}$, is formulated using an upstream scheme:

$$\begin{aligned} ADV_{(i,j)\to(i+1,j)} &= \begin{cases} u_{i,j} W_{i,j}, & \text{if } u_{i,j} \geq 0 \\ \\ u_{i,j} W_{i+1,j}, & \text{if } u_{i,j} < 0 \end{cases} \\ \\ ADV_{(i,j)\to(i,j+1)} &= \begin{cases} -v_{i,j} W_{i,j}, & \text{if } v_{i,j} \leq 0 \\ \\ -v_{i,j} W_{i,j+1}, & \text{if } v_{i,j} > 0 \end{cases} \end{aligned} \tag{3.120}$$

where i and j are the zonal and meridional indices of the grid box, which are counted from the west to the east and from the north to the south, respectively. The zonal and meridional advection rates $u_{i,j}$ and $v_{i,j}$ are defined at the interface of two grid boxes and depend on the slope of the orography:

$$\begin{aligned} u_{i,j} &= \frac{c}{\Delta x}\left[\frac{h_{i,j}-h_{i+1,j}}{\Delta x}\right]^{\alpha} \\ v_{i,j} &= \frac{c}{\Delta y}\left[\frac{h_{i,j+1}-hi,j}{\Delta y}\right]^{\alpha} \end{aligned} \tag{3.121}$$

where Δx and Δy are the distances between the grid points in the longitudinal and the meridional direction. h is the height of the orography, which is modified in order to omit local minima at land grid points. The empirical constants c and α are set to the values given by Sausen et al. (1994) for T21 resolution ($c = 4.2$ m/s and $\alpha = 0.18$).

3.5.4 Other Land Surface Parameter

Some additional quantities characterizing the land surface of each grid box need to be specified for use in the model. The land-sea mask and the orography are read from an external file. Optionally, this file may also include other climatological surface parameter: the global distribution of the surface roughness length z_0, a background albedo $\mathcal{R}_S^{clim}$, a glacier mask for permanent ice sheets, the bucked size for the soil water W_{max} (see section above) and a climatological annual cycle of the soil wetness C_w^{clim} (which may be used instead of the computed C_w from Eq. 3.117. If there is no input for the particular field in the file, the parameter is set to be horizontal homogeneous with a specific value. The following defaults are used: $z_0 = 2$ m, $\mathcal{R}_S^{clim} = 0.2$, no glaciers, $W_{max} = 0.5$ and $C_w^{clim} = 0.25$.

For snow covered areas, the background albedo is modified to give the actual albedo $\mathcal{R}_S$ which is used in the radiation scheme. For points, which are not covered by glaciers, $\mathcal{R}_S$ is given by

$$\mathcal{R}_S = \mathcal{R}_S^{clim} + (\mathcal{R}_S^{snow} - \mathcal{R}_S^{clim})\,\frac{z_{snow}}{z_{snow}+0.01} \tag{3.122}$$

where z_{snow} is the snow depth, and the albedo of the snow, $\mathcal{R}_S^{snow}$, depends on the surface temperature T_S

$$\mathcal{R}_S^{snow} = \mathcal{R}_{max}^{snow} + (\mathcal{R}_{min}^{snow} - \mathcal{R}_{max}^{snow})\,\frac{T_S - 263.16}{10} \tag{3.123}$$

with $\mathcal{R}_{min}^{snow} \le \mathcal{R}_S^{snow} \le \mathcal{R}_{max}^{snow}$ and default values $\mathcal{R}_{min}^{snow} = 0.4$ and $\mathcal{R}_{max}^{snow} = 0.8$.
For glaciers, $\mathcal{R}_S$ is given by $\mathcal{R}_S^{snow}$ from Eq. 3.123 but with a default $calR_{min}^{snow} = 0.6$.
The surface specific humidity q_S is given by the saturation specific humidity at T_S:

$$q_S = q_{sat}(T_S) \tag{3.124}$$

where $q_{sat}(T_S)$ is computed from Eq. 3.78.

3.6 Sea Surface

Sea surface temperatures T_{sea}, sea ice distributions c_{ice} and surface temperatures over sea ice T_i are provided by the ocean and sea ice modules (Section HEIKO). From these quantities, the following additional parameter are computed which enter the atmospheric parameterizations.

The prescribed surface albedo $\mathcal{R}_{\mathcal{S}}$ for open water is set to a default value of 0.069. For sea ice $\mathcal{R}_S$ is given as a function of the ice surface temperature T_i:

$$\mathcal{R}_S = \min\left(\mathcal{R}_S^{max},\, 0.5 + 0.025\,(273. - T_i)\right) \tag{3.125}$$

where the prescribed maximum sea ice background albedo $\mathcal{R}_S^{max}$ is set to a default value of 0.7.

The surface specific humidity q_S is given by the saturation specific humidity at the surface temperature T_S which is either T_{sea} or T_i:

$$q_S = q_{sat}(T_S) \tag{3.126}$$

where $q_{sat}(T_S)$ is computed from Eq. 3.78. The wetness factor C_w which enters the calculation of the surface evaporation (Eq. 3.4) is set to 1.

The roughness length z_0 over sea ice is set to a constant value of $z_0 = 0.001$ m. Over open water, z_0 is computed from the Charnock (1955) formula:

$$z_0 = C_{char}\frac{u_*^2}{g} \tag{3.127}$$

with a minimum value of $1.5 \cdot 10^{-5}$ m. C_{char} denotes the Charnock constant and is set to 0.018. g is the gravitational acceleration. The friction velocity u_* is calculated from the surface wind stress at the previous time level:

$$u_* = \sqrt{\frac{|F_u, F_v|}{\rho}} \tag{3.128}$$

where $|F_u, F_v|$ is the absolute value of the surface wind stress computed from Eq. 3.4 and ρ is the density.

3.7 References

Berger, A., 1978a: A simple algorithm to compute long-term variations of daily insolation. Institute of Astronomy and Geophysic, Universite Catholique de Louvain, **Contribution 18**, Louvain-la-Neuve, Belgium.

Berger, A., 1978b: Long-term variations of daily insolation and quaternary climatic change. *J. Atmos. Sci.*, **35**, 2362- 2367.

Blackadar, A. K., 1962: The vertical distributionof wind and turbulent exchange in a neutral atmosphere. *J. Geophys. Res.*, **67**, 3095-3102.

Boer, G. J., N. A. McFarlane, R. Laprise, J. Henderson and J.-P. Blanchet, 1984: The Canadian Climate Centre spectral atmospheric general circulation model. *Atmosphere-Ocean*, **22**, 397-429.

Charnock, M., 1955: Wind stress on a water surface. *Q. J. R. Meteorol. Soc.*, **81**, 639-640.

Chou, M.-D., M. J. Suarez, X.-Z. Liang and M. M. H. Yan, 2001 (Revised 2002): A thermal infrared radiation parameterization for atmospheric studies. *Technical Report Series on Global Modelling and Data Assimilation, M. J. Suarez Ed.*, **NASA/TM-2001-104606, Vol. 19**, 55pp.

Green, A. E. S., 1964: Attenuation by ozone and the earth's albedo in the middle ultraviolet. *AAppl. Opt.*, **3**, 203-208.

Katayama, A., 1972: A simplified scheme for computing radiative transfer in the troposphere. Department of Meteorology, *Tech. Report*, **No. 6**, University of California, Los Angeles, CA, 77 pp.

Kiehl, J. T., J. J. Hack, G. B. Bonan, B. A. Boville, B. P. Briegleb, D. L. Williamson and P. J. Rasch, 1996: Description of the NCAR Community Climate Model (CCM3). *NCAR Technical Note*, **NCAR/TN-420+STR**, 152pp.

Kuo, H. L., 1965: On formation and intensification of tropical cyclones through latent heat release by cumulus convection. *J. Atmos. Sci.*, **22**, 40-63.

Kuo, H. L., 1974: Further studies of the parameterization of the influence of cumulus convection on large-scale flow. *J. Atmos. Sci.*, **31**, 1232-1240.

Lacis, A. A., and J. E. Hansen, 1974: A parameterization for the absorption of solar radiation in the Earth's atmosphere. *J. Atmos. Sci.*, **31**, 118-133.

Laurson, L. and E. Eliasen, 1989: On the effects of the damping mechanisms in an atmospheric general circulation model. *Tellus*, **41A**, 385-400.

Louis, J. F., 1979: A parametric model of vertical eddy fluxes in the atmosphere. *Boundary Layer Meteorology*, **17**, 187-202.

Louis, J. F., M. Tiedtke and M. Geleyn, 1982: A short history of the PBL parameterisation at ECMWF. Proceedings, ECMWF workshop on planetary boundary layer parameterization, Reading, 25-27 Nov. 81, 59-80.

Lowe, P. R., 1977: An approximating polynomial for the computation of saturation vapour pressure. *J. Appl. Met.*, **16**, 100-103.

Manabe, S. and F. Möller, 1961: on the radiative equilibrium and heat balance of the atmosphere. *Mon Wea. Rev.*, **89**, 503-532.

Manabe, S., 1969: Climate and ocean circulation. I. The atmospheric circulation and the hydrology of the earth's surface. *Mon. Wea. Rev.*, **97**, 739-774.

Miller, M. J., A. Beljaars and T. N. Palmer, 1992: The sensitivity of the ECMWF model to the parameterization of evaporation from the tropical oceans. *J. Climate*, **5**, 418-434.

Rodgers, C. D., 1967: The use of emissivity in the atmospheric radiation calculation. *Q. J. R. Meteorol. Soc.*, **93**, 43-54.

Roeckner, E., K. Arpe, L. Bengtsson, S. Brinkop, L. Dümenil, M. Esch, E. Kirk, F. Lunkeit, M. Ponater, B. Rockel, R. Sausen, U. Schlese, S. Schubert and M. Windelband, 1992: Sim-

ulation of the present-day climate with the ECHAM-3 model: Impact of model physics and resolution. Max-Planck Institut für Meteorologie, **Report No. 93**, 171pp.

Sasamori, T., 1968: The radiative cooling calculation for application to general circulation experiments. *J. Appl. Met.*, **7**, 721-729.

Sausen, R., S. Schubert and L. Dümenil, 1994: A model of river runoff for use in coupled atmosphere-ocean models. *Journal of Hydrology*, **155**, 337-352.

Slingo, A., and J. M. Slingo, 1991: Response of the National Center for Atmospheric Research community climate model to improvements in the representation of clouds. *J. Geoph. Res.*, **96**, 341-357.

Stephens, G. L., 1978: Radiation profiles in extended water clouds. II: Parameterization schemes. *J. Atmos. Sci.*, **35**, 2123-2132.

Stephens, G. L., 1984: The parameterization of radiation for numerical weather prediction and climate models. *Mon. Wea. Rev.*, **112**, 826-867.

Stephens, G. L., S. Ackermann and E. A. Smith, 1984: A shortwave parameterization revised to improve cloud absorption. *J. Atmos. Sci.*, **41**, 687-690. Tiedtke, M., 1983: The sensitivity of the time-mean large-scale flow to cumulus convection in the ECMWF model. Proceedings of the ECMWF Workshop on Convection in *Large-Scale Models, 28 November-1 December 1983, European Centre for Medium-Range Weather Forecasts, Reading, England*, 297-316.

Chapter 4

Equations

4.1 Pressure coordinate

The primitive equations in the (λ, μ, p) -coordinates without scaling. That means D and $zeta$ in Appendix A and B have the units: s^-1, T is in K, p in Pa, ϕ in $m^2 s^{-2}$ and $\vec{\nu}$ in ms^{-1}.

Conservation of momentum (vorticity and divergence equation)

$$\frac{\partial \zeta}{\partial t} = -\vec{\nu} \cdot \bigtriangledown(\zeta + f) - \omega \frac{\partial \zeta}{\partial p} - (\zeta + f) \bigtriangledown \cdot \vec{\nu} + \vec{k} \cdot (\frac{\partial \vec{\nu}}{\partial p} \times \bigtriangledown \omega) + P_\zeta \tag{4.1}$$

$$\frac{\partial D}{\partial t} = \vec{k} \cdot \bigtriangledown \times (\zeta + f)\vec{\nu} - \bigtriangledown \cdot (\omega \frac{\partial \vec{\nu}}{\partial p}) - \bigtriangledown^2(\phi + \frac{\vec{\nu}^2}{2}) + P_D \tag{4.2}$$

Hydrostatic approximation (using the equation of state)

$$\frac{\partial \phi}{\partial p} = -\frac{1}{\rho} = -\frac{RT}{p} \tag{4.3}$$

Conservation of mass (continuity equation)

$$\bigtriangledown \cdot \vec{\nu} + \frac{\partial \omega}{\partial p} = 0 \tag{4.4}$$

Thermodynamic equation (J= diabatic heating per unit mass)

$$\frac{dT}{dt} = \frac{\omega}{c_p \rho} + \frac{J}{c_p} + P_T \tag{4.5}$$

4.2 Sigma-system

$\sigma = p/p_s$ ranges monotonically from zero at the top of the atmosphere to unity at the ground. For $\xi = x, y$ or t

$$(\frac{\partial}{\partial \xi})_p = \frac{\partial}{\partial \xi} - \sigma \frac{\partial \ln p_s}{\partial \xi} \frac{\partial}{\partial \sigma} \tag{4.6}$$

$$\frac{\partial}{\partial p} = \frac{\partial \sigma}{\partial p} \frac{\partial}{\partial \sigma} = \frac{1}{p_s} \frac{\partial}{\partial \sigma} \tag{4.7}$$

The vertical velocity in the p-coordinate system ω and in the new σ-coordinate system $\dot{\sigma}$ are given by [Phillips (1957)]

$$\omega = \frac{p}{p_s}[\vec{V}\cdot\nabla p_s - \int_0^\sigma \nabla\cdot p_s\vec{V}d\sigma] = p[\vec{V}\cdot\nabla\ln p_s] - p_s\int_0^\sigma Ad\sigma \tag{4.8}$$

$$\dot{\sigma} = \sigma\int_0^1 Ad\sigma - \int_0^\sigma Ad\sigma \tag{4.9}$$

with $A = D + \vec{V}\cdot\nabla\ln p_s = \frac{1}{p_s}\nabla\cdot p_s\vec{V}$.
The primitive equations in the (λ,μ,σ) -coordinates without scaling
Conservation of momentum (vorticity and divergence equation)

$$\frac{\partial\zeta}{\partial t} = \frac{1}{a(1-\mu^2)}\frac{\partial F_\nu}{\partial\lambda} - \frac{1}{a}\frac{\partial F_u}{\partial\mu} + P_\zeta \tag{4.10}$$

$$\frac{\partial D}{\partial t} = \frac{1}{a(1-\mu^2)}\frac{\partial F_u}{\partial\lambda} + \frac{1}{a}\frac{\partial F_\nu}{\partial\mu} - \bigtriangledown^2(E+\phi+T_0\ln p_s) + P_D \tag{4.11}$$

Hydrostatic approximation (using the equation of state)

$$\frac{\partial\phi}{\partial\ln\sigma} = -TR \tag{4.12}$$

Conservation of mass (continuity equation)

$$\frac{\partial\ln p_s}{\partial t} = -\frac{U}{a(1-\mu^2)}\frac{\partial\ln p_s}{\partial\lambda} - \frac{V}{a}\frac{\partial\ln p_s}{\partial\mu} - D - \frac{\partial\dot{\sigma}}{\partial\sigma} = -\int_0^1 (D+\vec{V}\cdot\nabla\ln p_s)d\sigma \tag{4.13}$$

Thermodynamic equation (J= diabatic heating per unit mass)

$$\frac{\partial T}{\partial t} = F_T - \dot{\sigma}\frac{\partial T}{\partial\sigma} + \kappa T[\vec{V}\cdot\nabla\ln p_s - \frac{1}{\sigma}\int_0^\sigma Ad\sigma] + \frac{J}{c_p} + P_T \tag{4.14}$$

$E = \dfrac{U^2+V^2}{2(1-\mu^2)}$
$F_u = (\zeta+f)V - \dot{\sigma}\dfrac{\partial U}{\partial\sigma} - \dfrac{RT}{a}\dfrac{\partial\ln p_s}{\partial\lambda}$
$F_\nu = -(\zeta+f)U - \dot{\sigma}\dfrac{\partial V}{\partial\sigma} - (1-\mu^2)\dfrac{RT}{a}\dfrac{\partial\ln p_s}{\partial\mu}$
$F_T = -\dfrac{U}{a(1-\mu^2)}\dfrac{\partial T}{\partial\lambda} - \dfrac{V}{a}\dfrac{\partial T}{\partial\mu}$
$A = D + \vec{V}\cdot\nabla\ln p_s = \frac{1}{p_s}\nabla\cdot p_s\vec{V}$.

4.3 Matrix $\boldsymbol{B}$

For the implicit scheme, fast (linear) gravity modes and the slower non-linear terms are separated.

$$\frac{\partial D}{\partial t} = N_D - \bigtriangledown^2(\phi + T_0 \ln p_s)$$

$$\frac{\partial \ln p_s}{\partial t} = N_p - \int_0^1 D d\sigma$$

$$\frac{\partial T'}{\partial t} = N_T - [\sigma \int_0^1 D d\sigma - \int_0^\sigma D d\sigma] \frac{\partial T_0}{\partial \sigma} + \kappa T_0 [- \int_0^\sigma D d \ln \sigma]$$

$$\frac{\partial \phi}{\partial \ln \sigma} = -T$$

The set of differential equations are approximated by its finite difference analogues using the notation (for each variable D, T, $\ln p_s$, and ϕ)

$$\overline{Q}^t = 0.5(Q^{t+\Delta t} + Q^{t-\Delta t}) = Q^{t-\Delta t} + \Delta t \delta_t Q$$

and

$$\delta_t Q = \frac{Q^{t+\Delta t} - Q^{t-\Delta t}}{2\Delta t}$$

The hydrostatic approximation using an angular momentum conserving finite-difference scheme is solved at half levels

$$\phi_{r+0.5} - \phi_{r-0.5} = T_r \cdot \ln \frac{\sigma_{r+0.5}}{\sigma_{r-0.5}}$$

Full level values of geopotential are given by

$$\phi_r = \phi_{r+0.5} + \alpha_r T_r \text{ with } \alpha_r = 1 - \frac{\sigma_{r-0.5}}{\Delta \sigma_r} \ln \frac{\sigma_{r+0.5}}{\sigma_{r-0.5}} \text{ and } \Delta \sigma_r = \sigma_{r+0.5} - \sigma_{r-0.5}$$

Now, the implicit formulation for the divergence is derived using the conservation of mass, the hydrostatic approximation and the thermodynamic equation at discrete time steps

$$\delta_t D = N_D - \bigtriangledown^2(\overline{\phi}^t + T_0[\ln p_s^{t-\Delta t} + \Delta t \delta_t \ln p_s])$$

$$\delta_t \ln p_s = N_p - L_p[D^{t-\Delta t} + \Delta t \delta_t D]$$

$$\overline{\phi - \phi_s}^t = L_\phi[T^{t-\Delta t} + \Delta t \delta_t T]$$

$$\delta_t T' = N_T - L_T[D^{t-\Delta t} + \Delta t \delta_t D]$$

The set of differential equations for each level $k(k = 1, .., n)$ written in vector form leads to the matrix $\mathcal{B}$ with n rows and n columns. The matrix $\mathcal{B} = \mathcal{L}_\phi \mathcal{L}_T + \vec{T}_0 \vec{L}_p = \mathcal{B}(\sigma, \kappa, \vec{T}_0)$ is constant in time. The variables $\vec{D}, \vec{T}, \vec{T}', \vec{\phi} - \vec{\phi}_s$ $\vec{N}_D$ and $\vec{N}_T$ are represented by column vectors with values at each level. L_p, L_T and L_ϕ contain the effect of the divergence (or the gravity waves) on the surface pressure tendency, the temperature tendency and the geopotential.

$\vec{L}_p = (\Delta\sigma_1, ..., \Delta\sigma_n)$ is a row vector with $\Delta\sigma_n = \sigma_{n+0.5} - \sigma_{n-0.5}$.

$$\mathcal{L}_\phi = \begin{pmatrix} 1 & \alpha_{21} & \alpha_{31} & \cdots & \alpha_{n1} \\ 0 & \alpha_{22} & \alpha_{32} & \ddots & \vdots \\ \vdots & \vdots & \vdots & \ddots & \vdots \\ 0 & 0 & \cdots & 0 & \alpha_{nn} \end{pmatrix}$$

For $i = j : \alpha_{jj} = 1 - [\frac{\sigma_{j-0.5}}{\sigma_{j+0.5} - \sigma_{j-0.5}}(\ln \sigma_{j+0.5} - \ln \sigma_{j-0.5})]$

$i > j : \alpha_{ij} = \ln \sigma_{j+0.5} - \ln \sigma_{j-0.5}$

$i < j : \alpha_{ij} = 0.$

$$\mathcal{L}_T = \begin{pmatrix} \kappa(T_0)_1\alpha_{11} & \kappa(T_0)_1\alpha_{21} & \cdots & \kappa(T_0)_1\alpha_{n1} \\ \kappa(T_0)_2\alpha_{12} & \kappa(T_0)_2\alpha_{22} & \ddots & \vdots \\ \vdots & \vdots & \ddots & \vdots \\ \kappa(T_0)_n\alpha_{1n} & \kappa(T_0)_n\alpha_{2n} & \cdots & \kappa(T_0)_n\alpha_{nn} \end{pmatrix} + \begin{pmatrix} \gamma_{11} & \gamma_{21} & \gamma_{31} & \cdots & \gamma_{n1} \\ \gamma_{12} & \gamma_{22} & \gamma_{32} & \ddots & \vdots \\ \vdots & \vdots & \vdots & \ddots & \vdots \\ \gamma_{1n} & \gamma_{2n} & \cdots & \cdots & \gamma_{nn} \end{pmatrix}$$

$\tau_{ij} = \kappa(T_0)_j\alpha_{ij} + \gamma_{ij}$ with $\Delta T_{n+0.5} = (T_0)_{n+1} - (T_0)_n$

for $j = 1$ and
$i = j$: $\gamma_{jj} = \frac{1}{2}[\Delta T_{0.5}(\sigma_1 - 1)]$

$i > j$: $\gamma_{ij} = \frac{1}{2}\Delta\sigma_i[\Delta T_{0.5}\sigma_1]$

for $j > 1$ and
$i = j$: $\gamma_{jj} = \frac{1}{2}[\Delta T_{j-0.5}\sigma_{j-0.5} + \Delta T_{j+0.5}(\sigma_{j+0.5} - 1)]$

$i < j$: $\gamma_{ij} = \frac{\Delta\sigma_i}{2\Delta\sigma_j}[\Delta T_{j-0.5}(\sigma_{j-0.5} - 1) + \Delta T_{j+0.5}(\sigma_{j+0.5} - 1)]$

$i > j$: $\gamma_{ij} = \frac{\Delta\sigma_i}{2\Delta\sigma_j}[\Delta T_{j-0.5}\sigma_{j-0.5} + \Delta T_{j+0.5}\sigma_{j+0.5}]$

Part II

Ocean: Mixed Layer

Chapter 5

Slab Ocean Model

The slab ocean model consists of a prognostic equation at each ocean point for the oceanic mixed-layer temperature T_{mix}. The prognostic equation for T_{mix} is given by

$$\frac{dT_{mix}}{dt} = \frac{Q_A + Q_O}{\rho_w c_{p_w} h_{mix}} \tag{5.1}$$

where ρ_w (=1030kg/m^3) is the density and c_{pw} (=4180J/kg/K) the heat capacity of ocean water. h_{mix} is a prescribed ocean mixed layer depth (default = 50m). Q_A denotes the net atmospheric heat flux into the ocean which consists of the net solar and long wave radiation and the sensible and latent heat fluxes.

The ocean mixed layer heat flux (Q_O) represents the oceanic transport and the deep water exchange. Commonly Q_O is prescribed from monthly mean data which are obtained from climatologies of the uncoupled model by computing

$$Q_O = < Q_A^u > - < \frac{dT_{mix}}{dt} \rho_w c_{p_w} h_{mix} > \tag{5.2}$$

where $< Q_A^u >$ and $< dT_{mix}/dt >$ are the climatological (monthly) averages of the net atmospheric heat flux and the mixed layer temperature tendency, respectively, both taken from the uncoupled (i.e. prescribed SST) simulation.

In addition to a prescribed oceanic heat transport, horizontal and vertical diffusion can be switched on optionally. In the case of vertical diffusion a user defined number n of layers with prescribed thicknesses h_{mix}^n are coupled via diffusion

$$\frac{\partial T_{mix}}{\partial t} = \frac{\partial}{\partial z} \left(K_v \frac{\partial T_{mix}}{\partial z} \right) \tag{5.3}$$

with the (level dependend) diffusion coefficient K_v (set to a default value of 0.0001m^2/s for all levels). The equation is solved using a back-substitution method.

Horizontal diffusion of T_{mix} is given by

$$\frac{\partial T_{mix}}{\partial t} = K_h \nabla^2 T_{mix} \tag{5.4}$$

for each level. The default value of K_h is 1000m^2/s.

Part III

Biosphere: SIMBA

Chapter 6

Dynamic Vegetation

A simple terrestrial dynamic global vegetation model (DGVM), Simulator for Biospheric Aspects (SimBA), is used to obtain the following land surface variables for non-glaciated grid cells: surface albedo A, the roughness length z_0, a surface conductance factor for the latent heat flux C_w, and a "bucket" depth for the soil, W_{max}. These land surface variables depend on SimBA variables– the latter of which ultimately depend on the following three (global) variables: soil moisture content (W_{soil}), snow depth (z_{snow}), and vegetative biomass (BM). Of these three variables, vegetative biomass has the greatest importance within SimBA.

6.1 Equations for SimBA Variables

Vegetative biomass (BM) depends on net primary productivity as given in SimBA's fundamental governing equation:

$$\frac{\partial BM}{\partial t} = NPP - \frac{BM}{\tau_{veg}} \tag{6.1}$$

where τ_{veg} is the residence time of the vegetative carbon and equals 10 years, and NPP (net primary productivity) is approximated as $0.5 * GPP$.

The approximation $NPP = 0.5 * GPP$ is briefly justified in [Kleidon (2006)], but some recent studies find that NPP/GPP can deviate considerably from 0.5 ([DeLucia et al. (2007)]; [Zhang et al. (2009)]). Nevertheless, the NPP/GPP = constant parameterization is attractively simple, and it has been assumed by widely-used productivity models such as CASA and FOREST-BGC ([DeLucia et al. (2007)]). A scheme for heterotrophic respiration is currently included in the model as a diagnostic only. The gross primary production formulation is detailed in the next subsection.

6.1.1 Gross Primary Production

GPP is calculated as the minimum of a water-limited rate and a light-limited rate. (That is, $GPP = min(GPP_{light}, GPP_{water}.)$ This approach originates in a crop model ([Monteith et al. (1989)]) which was later adapted for forest canopies ([Dewar (1997)]).

Light-limited Gross Primary Production

The light-limited rate, GPP_{light} follows a light-use efficiency approach (e.g. see [Yuan et al. (2007)]) as follows:

$$GPP_{light} = \epsilon_{luemax} * \beta(CO_2) * f(T_{sfc}) * fPAR * SW\downarrow \tag{6.2}$$

where ϵ_{luemax} is a globally-constant maximum light use efficiency parameter = $3.4{*}10^{-10}$ kgC/J, $\beta(CO_2)$ represents a logarithm-based "beta" factor effect on productivity for when CO_2 concentration deviates from the reference value of 360ppmv (see below), $f(T_{sfc})$ is a temperature limitation function (defined below) which lowers productivity for cold temperatures, $fPAR$ is the fraction of photosynthetically active radiation that is absorbed by green vegetation (see below), and $SW\downarrow$ is the downward flux of shortwave radiation at the surface (in W/m^2).

In equation (6.2), the first term on the right hand side, ϵ_{luemax}, is the light use efficiency with respect to the absorbed total shortwave broadband radiation. The value of $3.4 * 10^{-10}$ kgC per J (of fPAR * $SW\downarrow$) is derived from the maximum light use efficiency value of the CASA model, 0.389 gC MJ^{-1} of APAR [absorbed photosynthetically active radiation] ([Potter et al. (1993)];[Field et al. (1995)]) by using the commonly-used approximations GPP = 0.5*NPP and $SW\downarrow = 0.5$ * PAR [photosynthetically active radiation] (at top of the canopy). (Both approximations are made in the CASA model ([Potter et al. (1993)];[Field et al. (1995)])). The equivalent ϵ_{luemax} value in SimBA would be $3.89 * 10^{-10}$ kgC/J, but this is lowered to $3.4 * 10^{-10}$ kgC/J to account for the lack of an optimum growing temperature in SimBA, since the lack of such an optimum causes light-limited productivity to be slightly overestimated for most regions.

The second term in equation (6.2), $\beta(CO_2)$, is taken from ([Harvey (1989)]), but incorporates carbon compensation point as follows:

$$\beta(CO_2) = 1 + \max\left(0, BF * \ln\left(\frac{CO_2 - CO_{2,comp}}{CO_{2,ref} - CO_{2,comp}}\right)\right) \tag{6.3}$$

where BF = the carbon dioxide sensitivity or "beta" factor, $CO_{2,ref}$ = 360ppmv, and $CO_{2,comp}$ = the light compensation point (in ppmv) (set to zero by default).

The third term in equation (6.2), $f(T_{sfc})$, is as follows:

$$f(T_{sfc}) = \begin{cases} 0 & \text{if } T_{sfc} \leq 0\,^{\circ}\text{C} \\ \frac{T_{sfc}}{T_{crit}} & \text{if } 0 < T_{sfc} < T_{crit} \\ 1 & \text{if } T_{sfc} \geq T_{crit} \end{cases} \tag{6.4}$$

where T_{sfc} is the surface temperature in °C, and T_{crit} is the "critical" temperature (set to 5 °C) by default) at which temperature is no longer limiting to productivity.

The fourth term in equation (6.2), fPAR, is also referred to as "vegetation cover" (f_{veg}) in the model. "fPAR" refers to fraction of photosynthetically active radiation (PAR) that is absorbed by photosynthesizing parts (i.e. green leaves) of plants. (PAR is the fraction of incoming solar radiation that is in wavelengths usable for photosynthesis.) In a Beer's Law approach, fPAR can be approximated as a function of the leaf area index (LAI):

$$fPAR = 1 - e^{-k_{veg} * LAI} \tag{6.5}$$

where k_{veg} is a light extinction coefficient (set to 0.5 by default). This same approach is followed in the forest canopy and crop models on which SimBA is based ([Monteith et al. (1989)]; [Dewar (1997)]), and it is also used in the formulation of snow-free surface albedo in the ECHAM5 GCM ([Rechid et al. (2009)]) as well as in SimBA (see section below on surface albedo).

Water-limited Gross Primary Production

The water-limited rate, GPP_{water}, whose equation we derive here, is based on the equivalent formulation in the forest canopy model of [Dewar (1997)] and follows a "big leaf"-diffusivity approach. Diffusions of CO_2 and H_2O between leaf and atmosphere are proportional to the

concentration gradient between leaf intercellular air and atmosphere times the respective diffusivities of these gases. In our "big leaf" model, the canopy is treated as if it were a large single leaf that is well coupled to the atmosphere. Such strong leaf-atmosphere coupling permits us to neglect the leaf boundary layer conductance as compared to the stomatal conductance. Following the appendix section of [Dewar (1997)], we can now write an equation for water-use efficiency at the leaf scale, q_{leaf}:

$$q_{leaf} = \frac{c_a}{1.6VPD}(1 - \frac{c_i}{c_a}) \tag{6.6}$$

where c_i is the intercellular CO_2 concentration, c_a is the atmospheric CO_2 concentration, VPD = the vapor pressure deficit between the (presumed) saturated leaf surface and atmosphere, and the "1.6" term represents the difference in diffusivity between CO_2 and H_2O due to their differing molecular weights. Here, the units are assigned as follows: q_{leaf} is in $\frac{molC}{molH_2O}$; c_i and c_a are in Pa CO_2; VPD is in Pa H_2O; and the "1.6" term has units of $\frac{\frac{molH_2Om^{-2}s^{-1}}{PaH_2O/Paair}}{\frac{molCO_2m^{-2}s^{-1}}{PaCO_2/Paair}} = \frac{PaCO_2}{PaH_2O}\frac{molH_2O}{molCO_2} = \frac{PaCO_2}{PaH_2O}\frac{molH_2O}{molC}$ (where "Pa air" is pascals of total atmospheric pressure, and where the last equality holds because there is one mole of carbon in each mole of CO_2).

Equation (6.6) can be written as mass- rather than mole-based water-use efficiency by multiplying the right hand side by a conversion factor of $\frac{12kgC/1000molC}{18kgH_2O/1000molH_2O}$, i.e. by $\frac{2}{3}\frac{kgCmolH_2O}{kgH_2OmolC}$. We call the new left hand side "q_{mass}" (with units of $\frac{kgC}{kgH_2O}$):

$$q_{mass} = \frac{c_a}{1.6VPD}(1 - \frac{c_i}{c_a}) \tag{6.7}$$

Next, we make a simplifying assumption that $\frac{c_i}{c_a}$ has a constant value of 0.7 to get

$$q_{mass} = \frac{2}{3}\frac{0.3c_a}{1.6VPD} \tag{6.8}$$

It should be noted that the simplifying assumption that $\frac{c_i}{c_a}$ is constant is not entirely valid. Although early studies showed that the ratio is largely conserved as ambient CO_2 is varied (e.g. [Wong et al. (1979)]; [Polley et al. (1993)]), many recent studies have found significant variance of the ratio (e.g. from 0.54 to 0.95 ([Brooks et al. (1997)]), such that decreasing $\frac{c_i}{c_a}$ is associated with increasing light ([Brooks et al. (1997)]), increasing leaf-atmosphere vapor pressure deficit ([Morison and Gifford (1983)]), greater soil moisture stress ([Turnbull et al. (2002)]), and higher canopy position ([Brooks et al. (1997)]). In addition, C_4 plants tend to have lower values than C_3 plants (e.g. see [Bunce (2005)]), which should thus cause SimBA to underestimate productivity in climatic zones which favor C_4 plants (warm and dry areas). On the other hand, at least one other more sophisticated productivity model assumes a constant $\frac{c_i}{c_a}$ ([Knorr (2000)]).

We can now use the relation, $NPP_{water} = 0.5\ GPP_{water}$, and q_{mass}, water-use efficiency, from equation (6.8) to write a large scale expression for water-limited gross primary production (GPP_{water}) as follows:

$$GPP_{water} = 2\ q_{mass}\ T \tag{6.9}$$

where T = transpiration (in $kgH_2O\ m^{-2}s^{-1}$), and GPP_{water} has units of $kgCm^{-2}s^{-1}$.

Next, we assume, as is also done in the original MOSES land surface model for the no-wet canopy case ([Cox et al. (1999)]), that transpiration's contribution to total evapotranspiration (ET) equals the vegetative cover fraction, f_{veg}, i.e. that

$$T = ET * f_{veg} \tag{6.10}$$

(Recall that we define $f_{veg} = fPAR = 1 - e^{-kveg*LAI}$ in SimBA.)

Next, we substitute in equations (6.8) and (6.10) into equation (6.9); use the conversion $c_a = P * co2 * 10^{-6}$, where P and c_a are atmospheric pressure and atmospheric carbon dioxide partial pressure, respectively (in Pa), and where co2 is the atmospheric carbon dioxide concentration (in ppmv); and use a reference density for H_2O of 1000 kg m^{-3} to get our final form equation for water-limited gross primary production:

$$GPP_{water} = \frac{co2conv * P * f_{veg} * ET * (0.3 * co2)}{VPD} \tag{6.11}$$

where co2conv = 8.3 * 10^{-4}, ET is evapotranspiration (in $\frac{m^3}{m^2 s}$), and GPP_{water} is again in $kgCm^{-2}s^{-1}$.

The above GPP_{light} and GPP_{water} formulas rely on vegetative cover fraction (f_{veg}) (which equals fPAR), and f_{veg} is a function of LAI. The next subsection describes how these are derived in SimBA.

6.1.2 Vegetative Cover

The vegetative cover f_{veg} of the land surface, that is the fraction which is covered by green biomass (leaves), is computed as the minimum of an water-limited value $f_{veg,w}$ and a structurally limited value $f_{veg,s}$:

$$f_{veg} = \min\left(f_{veg,w}, f_{veg,s}\right) \tag{6.12}$$

The water-limited vegetation cover $f_{veg,w}$ is computed from the soil moisture W_{soil} as:

$$f_{veg,w} = f_{W_{soil}} \tag{6.13}$$

with the function $f_{W_{soil}}$ given by:

$$f_{W_{soil}} = \min\left(1, \max\left(0, \frac{W_{soil}/W_{max}}{W_{crit}}\right)\right) \tag{6.14}$$

where $W_{crit} = 0.25$ and W_{max} is the biomass-dependent soil "bucket" depth (see below for derivation). This water limitation function, $f_{W_{soil}}$, is motivated by the fact that water stress for plants sets in at a critical value W_{crit}. For simplicity, a fractional water content is used rather than a specific matric potential which would reflect the permanent wilting point. Other land surface models use a similar approach (e.g. [Albertson and Kiely (2001)])

The structurally limited vegetation cover $f_{veg,s}$ is obtained from a structurally limited maximum leaf area index LAI_m as follows:

$$f_{veg,s} = 1 - \exp\left(-k_{veg}\, LAI_m\right) \tag{6.15}$$

which is sustained with the present amount of biomass:

$$LAI_m = 0.1 + \frac{2}{\pi} * LAI_{max} * atan(c_{veg_l} * BM) \tag{6.16}$$

where LAI_{max} represents the theoretical LAI that is approached as biomass becomes infinitely large, and with the values for $\text{LAI}_{max} = 9$ and $\text{c}_{veg_l} = 0.25$ giving the best fit to the old scheme used in earlier versions of SimBA for mid to high biomass (BM) values, while maintaing realism for low BM values. (See notes at end of section on forest cover for more info on how LAI parameterization was developed.)

$LAI = -\frac{\ln(1-f_{veg})}{k_{veg}}$ inputs back the effect of water limitation to LAI. As a final note, in the scheme presented here, LAI follows drought-deciduous phenology, but it does not follow winter-deciduous phenology.

6.1.3 Forest Cover

Forest cover is an influential variable in the model. In SimBA, forest cover refers to non-prostrate woody vegetation which sticks out above the snow pack. Only forest cover contributes to surface roughness, and only forest cover lowers the snow-covered surface albedo relative to that of snow-covered bare soil. Non-forested but vegetated land acts the same as bare soil with respect to surface roughness and snow-covered albedo.

Forest cover (F) is parameterized as follows:

$$F = 0.1 + \max(0, \frac{atan(BM - c_{veg_a}) - atan(c_{veg_d})}{0.5\pi - atan(c_{veg_d})}) \tag{6.17}$$

where $c_{veg_a} + c_{veg_d} = f_{crit}$, where f_{crit} is defined as the biomass threshold at which forest cover begins to rise above zero.

c_{veg_a} and c_{veg_d} are currently set at 2.9 and -1.9, respectively, and thus $f_{crit} = 1.0$ kg m^{-2}. c_{veg_a} is chosen to be near 3.0, which was the analogous value for the previous version of SimBA, thus giving an excellent fit between new and old forest cover parameterizations for biomass values above 3 kg m^{-2}.

How f_{crit} Was Chosen

Based on NPP and ecosystem type model data ([McGuire et al. (1992)]; [Cramer et al. (1999)]), it was estimated that woody shrub cover begins to occur at circa 100 g per m^2 per year of NPP in the real world, which equals 1 kg of biomass per m^2 in Simba under steady state conditions. This is a rough estimate, because forest cover is not solely a function of NPP.

More on the Basis for the Biomass-LAI and Biomass-forest Cover Relationships

The relationships were based more on NPP than on biomass. NPP data from [McGuire et al. (1992)] and [Cramer et al. (1999)] was converted into biomass data by using the steady state approximation $NPP \approx \frac{BM}{\tau_{veg}}$, which is obtained when the LHS of equation (6.1) is approximately 0 over long time scales. Forest cover and LAI were related by using the land surface dataset for the ECHAM GCM ([Hagemann (2002)]). Note that [Hagemann (2002)] apparently does not consider woody shrub cover to be partial forest cover, as does SimBA, and this was taken into account in creating the two formulations. Finally, LAI data for some arctic and mountain ecosystems ([Bliss et al. (1981)], p.195 and p.219) was also used to calibrate this part of the model.

6.2 Derivation of Land Surface Parameters

6.2.1 Soil Water Holding Capacity

We informally refer to it here as soil "bucket" depth. The general idea behind this formulation is that the bucket depth increases as the root biomass increases. This dependence on root biomass has been incorporated into other simple land surface schemes (e.g. ENTS for the GENIE climate system model ([Williamson et al. (2006)])).

The non-linear relationship between biomass and bucket depth (W_{max}) is due to the non-linear dependence of an intermediate variable, Vsoil, on biomass. The Vsoil-biomass relationship was originally designed to be perfectly analogous to the forest cover-biomass relationship, except for the former's using root biomass and the latter's using "shoot" biomass. This updated version of SimBA maintains essentially the same Vsoil-biomass relationship, except that now

it depends on total biomass. (Note: the code can be easily modified to account for root-shoot partitioning different than the implicit 0.5 value.) Here is the Vsoil-biomass equation:

$$Vsoil = \min(1.0, \max(0, \frac{atan(BM - c_{veg_f}) - atan(-c_{veg_f})}{0.5\pi - atan(-c_{veg_f})})) \tag{6.18}$$

where c_{veg_f} is set to 3.0 by default.

Next, soil bucket depth, W_{max} depends linearly on Vsoil as follows:

$$W_{max} = W_{max_{max}} * Vsoil + W_{max_{min}} * (1 - Vsoil) \tag{6.19}$$

where $W_{max_{max}} = 0.5$ is the theoretical soil bucket depth as biomass becomes infinitely large and $W_{max_{min}} = 0.05$ is the soil bucket depth when biomass = 0 kg m^{-2} (i.e. for bare soil). Each bucket depth has a unit of meters in the model, and the given values for $W_{max_{max}}$ and $W_{max_{min}}$ are taken from [Kleidon (2006)].

6.2.2 Surface Albedo

Surface albedo is first calculated for snow-free conditions, and then it is modified if there is snow. Solar zenith angle dependence, diffuse-direct radiation distinction, and the dependence of bare soil albedo on soil moisture content are all neglected.

Snow-free Surface Albedo

This formulation is identical to that used in ECHAM5 ([Rechid et al. (2009)]) and is as follows:

$$A_{snow-free} = A_{fully-leaved} * f_{veg} + A_{bare} * (1 - f_{veg}) \tag{6.20}$$

where "A" denotes albedo; "fully-leaved" and "bare" denote conditions of infinite LAI and zero LAI, respectively; and f_{veg} is vegetation cover (as before) $= 1 - e^{-k_{veg} * LAI}$, where k_{veg} is -0.5 as before. $A_{fully-leaved}$ and A_{bare} are currently set to 0.12 and 0.30, respectively.

It is important to note that snow-free albedo depends only on leaf area index (LAI) and not on forest cover. Stems and branches, etc., are tacitly assumed to have the same albedo as bare soil, 0.3.

Surface Albedo when Snow is Present

The grid cell is divided up into a forest-covered part and non-forest covered part. Non-forest cover is a mixture of prostrate vegetation (e.g. grass, non-shrubby tundra) and bare soil. The albedo of snow-free non-forest cover is mixed in with that of deep snow concurrent with the snow depth as follows:

$$A_{NF} = A_{NF_{snow-free}} + (A_{snow} - A_{NF_{snow-free}}) \frac{snowdepth}{snowdepth + 0.01} \tag{6.21}$$

where "NF" denotes non-forest cover, A_{snow} is the albedo of deep snow, and snowdepth is in meters. Note: the albedo of the snow-free non-forest cover is tacitly taken to equal the albedo of the entire grid cell under snow-free conditions.

Deep snow albedo, A_{snow}, lowers with increasing surface temperature (T_{sfc}) as follows:

$$A_{snow} = \begin{cases} A_{snow_{max}} & \text{if } T_{sfc} \leq -10\,^{\circ}\text{C} \\ A_{snow_{min}} + (A_{snow_{max}} - A_{snow_{min}})(\frac{T_{sfc}}{-10\,^{\circ}\text{C}}) & \text{if } -10\,^{\circ}\text{C} < T_{sfc} < 0\,^{\circ}\text{C} \\ A_{snow_{min}} & \text{if } T_{sfc} = 0\,^{\circ}\text{C} \end{cases} \tag{6.22}$$

where $A_{snow_{max}} = 0.8$ and $A_{snow_{min}} = 0.4$.

Forest cover (again denoted by "F") is modeled to protrude from the snow pack and mask the snow beneath it. For simplicity, the forest-covered portion of the grid cell is assigned the same albedo, $A_{F_{snow}}$, regardless of surface temperature or the amount of snow accumulation. $A_{F_{snow}}$ is assigned a default value of 0.20 in the model. Earlier versions of SimBA had $A_{F_{snow}} = 0.35$. The lower value of 0.20 has been adopted for a number of reasons: it is used in the ECHAM GCM for fully snow-covered evergreen forests ([Roesch et al. (2001)]; [Roesch and Roeckner (2006)]); and it is closer to satellite ([Gao et al. (2005)]) and field ([Betts and Ball (1997)]) measurement values, particularly when the trees are not cold winter-deciduous (as is the case in SimBA).

Finally, the albedo "A" for the entire grid cell, is taken to be the linear combination of the respective albedos for forest-covered (F) and non-forest-covered (NF) fractions:

$$A = A_{F_{snow}} * F + A_{NF} * (1 - F) \tag{6.23}$$

6.2.3 Surface Conductance

Also denoted as "rhs" or as "surface wetness" within the model, we denote it here as "C_w".

$$C_w = pgs * f_{W_{soil}} \tag{6.24}$$

where $f_{W_{soil}}$ is taken from equation (6.14) and represents a water stress factor due to reduced soil moisture content, and pgs represents the surface conductance achieved under non-water-stressed conditions. The default value for pgs in the model is 1.0. Finally, as a correction from previous versions of SimBA, C_w is set to 1.0 regardless of $f_{W_{soil}}$ when snowcover > 0, to take into account the presence of sublimatable snow at the surface.

6.2.4 Surface Roughness

Surface roughness is taken as a non-linear combination of roughness due to orography and roughness due to vegetation. As mentioned earlier, surface roughness due to vegetation is a function of forest cover only. Hence, no increase in surface roughness occurs as biomass goes from 0 kg m^{-2} to 1 kg m^{-2} (the value at which forest cover commences). We denote surface roughness due to vegetation as $z_{0,veg}$ and formulate it as follows:

$$z_{0,veg} = F * (z_{0,F}) + (1 - F)\,(z_{0,NF}) \tag{6.25}$$

where "F" and "NF" denote "forest cover" and "non-forest cover", respectively; $z_{0,NF}$=0.05 m, the vegetative surface roughness in the absence of forest cover; and $z_{0,F}$=2 m, the vegetative surface roughness when fully-forested (i.e. when F = 1).

Finally, surface roughness of a grid cell, z_0, is formulated as follows:

$$z_0 = \sqrt{{z_{0,veg}}^2 + {z_{0,oro}}^2} \tag{6.26}$$

where $z_{0,oro}$ is the surface roughness due solely to orography.

Part IV

Ice

Chapter 7

Model Description

The sea ice model is based on the zero layer model of [Semtner (1976)]. This model computes the thickness of the sea ice from the thermodynamic balances at the top and the bottom of the sea ice. The zero layer assumes the temperature gradient in the ice to be linear and eliminates the capacity of the ice to store heat. Nevertheless, it has been used successfully in areas where ice is mostly seasonal and thus relatively thin ($< 1\,\mathrm{m}$) [Beckmann and Birnbaum (2001)]. Thus, the model is expected to perform better in the Southern Ocean than in the Arctic, where multiyear, thick ice dominates. Sea ice is formed if the ocean temperature drops below the freezing point (set to 271.25 K) and is melted whenever the ocean temperature increases above this point. The prognostic variables are the sea ice temperature T_i, the ice thickness h_i and the ice concentration A, which in the present model is boolean: A given grid point is either ice free ($A = 0$) or ice covered ($A = 1$).

Freezing and melting of sea ice releases just the right amount of latent heat of fusion to close the energy balance with respect to the total heat flux Q in the mixed layer [Parkinson and Washington (1979

$$Q + \rho_i L_i \frac{\partial h_i}{\partial t} = 0, \tag{7.1}$$

where ρ_i is the density of sea ice and L_i denotes the latent heat of fusion of sea ice. Standard parameter values are given in Table 7.1. [Parkinson and Washington (1979)] Thus, the prognostic equation for the sea ice thickness is given as

$$\frac{\partial h_i}{\partial t} = \frac{-Q}{\rho_i L_i}. \tag{7.2}$$

It is assumed that melting of sea ice takes place from above only, while freezing takes place at the lower side of the ice floe.

Basic equations

In the presence of sea ice, the heat fluxes are defined as follows. The total heat flux $Q\,(\mathrm{W\,m^{-2}})$ is given as

$$Q = Q_a + Q_c + Q_o + \tilde{Q}, \tag{7.3}$$

where Q_a is the atmospheric heat flux, Q_c is the conductive heat flux through the ice, Q_o denotes the oceanic heat flux and $\tilde{Q}$ is the flux correction. The atmospheric heat flux

$$Q_a = \begin{cases} F_T + L + R_{s,\downarrow} + R_{s,\uparrow} + R_{l,\downarrow} + R_{l,\uparrow} & \text{if } T_s > T_f, \\ 0 & \text{if } T_s \leq T_f. \end{cases} \tag{7.4}$$

is the sum of sensible (F_T) and latent heat flux (L), the incoming and reflected short wave radiation ($R_{s,\downarrow}\, R_{s,\uparrow}$) and the long wave radiation (R_l). It is set to zero in the case of freezing, where the conductive heat flux applies (see below). The conductive heat flux through the ice

$$Q_c = \begin{cases} 0 & \text{if} \quad T_s > T_f, \\ \dfrac{\bar{\kappa}}{h_i + h_s}\,(T_s - T_f) & \text{if} \quad T_s \leq T_f. \end{cases} \tag{7.5}$$

is set to zero in the case of melting ice, as the ice melts at the top. $\bar{\kappa}$ is the mean conductivity of the sea ice floe and snow cover (with depth = h_s), computed as

$$\bar{\kappa} \;=\; \frac{\kappa_i h_i \;+ \kappa_s h_s}{h_i \;+ h_s}. \tag{7.6}$$

where κ_i and κ_s are the conductivities of sea ice and snow, respectively.

Commonly, the oceanic heat flux Q_o is parameterized in terms of the difference between the freezing temperature and the temperature of the ocean (mixed layer or deep ocean). Q_o sets an upper value for the ice thickness and, thus, limits the ice growth. However, to avoid artificial sources or sinks of heat the oceanic heat flux Q_o is set to zero in the present model. The ice thickness is limited to a prescribed value h_{max} (default = 9m) by setting $\bar{\kappa} = 0$ (i.e. $Q_c = 0$) for $h_i > h_{max}$.

The flux correction $\tilde{Q}$, if applied, is used to constrain the sea ice to a given distribution. It is obtained from the (monthly) climatology of an uncoupled (prescribed ice) simulation as

$$\tilde{Q} =< \rho_i L_i \frac{h_{clim} - h_i}{\Delta t} > \tag{7.7}$$

where h_{clim} is the (prescribed) climatological ice, Δt is the models time step and $< ... >$ denotes a climatological (monthly) average.

In the case of melting, the ice thickness may become negative if the energy available for melting is greater than needed to melt the present ice. Then, the surplus energy is heating the sea water, setting the surface temperature to

$$T_s \;=\; T_f \;- \frac{\rho_i \, L_i \, h_i}{\rho_w \, c_{p_s} \, h_{mix}}, \tag{7.8}$$

with $h_i < 0$.

Ice formation, freezing and melting

If the surface temperature of open ocean water is below the freezing point, sea ice is formed. The heat flux available for freezing is given as

$$Q_f \;=\; \frac{\rho_w \, c_{p_w} \, h_{ml}}{\Delta t}\,(T_s \;- T_f) \tag{7.9}$$

where ρ_w is the density of sea water, c_{p_w} is the specific heat of sea water and h_{ml} denotes the mixed layer depth. The thickness of the new formed ice sheet is calculated by setting $Q \;=\; Q_f \;+ \tilde{Q}$ in (7.1). Since the model differentiates only between no ice and full ice, a minimum ice thickness $h_{i,min}$ (default = 0.1m) needs to be present before a grid point is treated as ice covered (compactness $A = 1$). If h_i is less than $h_{i,min}$ the heat flux $Q_a + \tilde{Q}$ is used to build (or melt) ice. If $h_i > h_{i,min}$ a ice surface temperature (T_i) is computed (see below) and, if $T_i < T_f$, ice growths according to $Q_c + \tilde{Q}$. Ice is diminished if the ice surface temperature would be above freezing point.

Sea ice temperature

If a grid point is covered by sea ice (i.e. $h_i > h_{i,min}$) a sea ice surface temperature T_i is calculated from the energy balance at the ice surface. To avoid numerical problems (due to large changes of T_i within one time step), the energy balance equation is solved for an upper layer of the ice/snow column which has a heat capacity, $c_p^\star$, similar to that of $h_{i,min}$ pure ice ($c_p^\star = h_{i,min} c_{p_i} \rho_i$):

$$c_p^\star \frac{\partial T_i}{\partial t} - Q_b = 0 \Rightarrow \frac{\partial T_i}{\partial t} = \frac{Q_b}{c_p^\star} \tag{7.10}$$

where $Q_b = Q_a + Q_c$ with Q_a as defined in (7.4) and Q_c from (7.5). Eq. (7.10) is solved using an implicit formulation for the conductive heat flux Q_c.

Snow cover

If a grid point is covered by sea ice, snow fall is accumulated on top of the ice. Snow cover effects the albedo and the heat conductivity (according to eq. (7.6)). Snow is converted to sea ice if there is sufficient snow to suppress the ice/snow interface below the sea level. The conversion conserves mass. The new ice (h_i^{new}) and snow (h_s^{new}) thicknesses are given by:

$$h_i^{new} = \frac{\rho_s h_s + \rho_i h_i}{\rho_w} \tag{7.11}$$

$$h_s^{new} = \frac{\rho_w - \rho_i}{\rho_s} h_i^{new} \tag{7.12}$$

Where ρ_w and ρ_s are the densities of sea water and snow, respectively.

If the surface temperature is above freezing point, first the snow is melted, then the ice. Snow melts according to

$$\frac{dh_s}{dt} = \frac{Q_a}{\rho_s \, L_{sn}}, \tag{7.13}$$

where $\rho_s \, (\mathrm{kg/m^3})$ is the density of snow and $L_{sn} \, (\mathrm{J/kg})$ is the latent heat of fusion of snow. If the atmospheric heat flux is so large that it melts all the snow, then the remaining energy melts ice via (7.2).

Parameter	Symbol	Value	Reference
density of sea ice	ρ_i	$920\,\mathrm{kg\,m^{-3}}$	Kiehl et al. [1996, p. 139]
density of snow	ρ_s	$330\,\mathrm{kg\,m^{-3}}$	Kiehl et al. [1996, p. 139]
density of sea water[a]	ρ_w	$1030\,\mathrm{kg\,m^{-3}}$	
latent heat of fusion (ice)	L_i	$3.28 \times 10^5\,\mathrm{J\,kg^{-1}}$	Kiehl et al. [1996, p. 139]
latent heat of fusion (snow)	L_{sn}	$3.32 \times 10^5\,\mathrm{J\,kg^{-1}}$	Kiehl et al. [1996, p. 139]
heat conductivity in ice	κ_i	$2.03\,\mathrm{W\,m^{-1}\,K^{-1}}$	Kiehl et al. [1996, p. 139]
heat conductivity in snow	κ_s	$0.31\,\mathrm{W\,m^{-1}\,K^{-1}}$	Kiehl et al. [1996, p. 139]
specific heat of sea ice	c_{p_i}	$2070\,\mathrm{J\,kg^{-1}\,K^{-1}}$	Kiehl et al. [1996, p. 139]
specific heat of snow	c_{p_s}	$2090\,\mathrm{J\,kg^{-1}\,K^{-1}}$	Kiehl et al. [1996, p. 139]
specific heat of sea water	c_{p_w}	$4180\,\mathrm{J\,kg^{-1}\,K^{-1}}$	
freezing point of seawater [a]	T_f	271.25 K	
ocean water salinity	S_w	34.7 psu	

Table 7.1: Thermodynamic parameter values.[a] at S=34.7

Part V

Data

Chapter 8

Surface Data

A set of surface data is provided to serve as input for PlaSim in 3 resolutions: T21, T31 and T42. The file names begin with Nxxx, where xxx gives the number of latitudes of the respective resolution. The "mm" indicates monthly mean values (further explanation see below):

T21:

file name	**abbr.**	**unit**		**variable name**
N032_surf_0129.sra	sg	m^2/s^2		surface geopotential orography
N032_surf_0169.sra	tsa	K	mm	surface temperature accumulated
N032_surf_0172.sra	lsm	fract.		land sea mask
N032_surf_0173.sra	z0	m		roughness length
N032_surf_0174.sra	alb	fract.	mm	albedo (surface background albedo)
N032_surf_0199.sra	vegc	fract.	mm	fractional vegetation
N032_surf_0200.sra	lai		mm	leaf area index
N032_surf_0210.sra	sic	%	mm	sea ice cover
N032_surf_0212.sra	vegf	fract.		forest ratio
N032_surf_0229.sra	mrfc	m		maximum soil water holding (field) capacity
N032_surf_0232.sra	glac	fract.		glacier fraction
N032_surf_1730.sra	z0t	m		roughness length due to topography
N032_surf_1731.sra	z0v	m		roughness length due to vegetation and land use
N032_surf_1740.sra	albs	fract.		bare soil albedo
N032_surf_1741.sra	albv	fract.		albedo due to vegetation

T31:
file names begin with: N048

T42:
file names begin with: N064

The format of the files is "service ascii". They are opened as FORMATTED files and can be read as:

```
integer :: ih (8)
real    :: field (nlon,nlat)

open(filenr,file='N....sra',form='FORMATTED')
read(filenr,*) ih
read(filenr,*) field
```

As the files contain formatted data, any text editor could be used to view or change the data as well.
The data of tsa (code 169), alb (code 174), vegc (code 199), lai (code 200) and sic (code 210) are stored as 14 monthly mean fields (indicated by the "mm" in the table above): Jan to Dec are months 1 to 12 with Dec duplicated as month 0 and Jan duplicated as month 13.
All other files contain one yearly mean field.

8.1 Source

The data are obtained from four different sources:

8.1.1 codes: 174, 199, 200, 212, 229, 232, 1731

These data are obtained from the LSP dataset of the U.S. Geological Survey, which is based on a 1km global distribution of major ecosystem types.
They are part of a dataset provided by Stefan Hagemann, MPI Hamburg in T21, T31 and T42 resolution. A detailed description can be found in two MPI scientific reports
[Hagemann et al. (1999)] and [Hagemann (2002)].
The values refer to the land part of the grid box.

8.1.2 codes: 173, 1730 and 129, 172

The data of the "roughness length due to topography" and therefore the total roughness length as well are not included in the above mentioned dataset. $z0_t$ (code 1730) was calculated by MPI Hamburg (and provided by Uwe Schulzweida) as ECHAM input from the GTOPO30 dataset of the U.S. Geological Survey (`http://eros.usgs.gov`), which is regularly spaced at 30-arc seconds (app. 1km). The method is described in [Tibaldi and Geleyn, (1981)].
$z0$ (code 173) is calculated using:

$$z0 = \sqrt{z0_t^2 + z0_v^2} \tag{8.1}$$

according to [Hagemann et al. (1999)].
The surface geopotential (= $g*$ Topography [m]) and the land sea mask are also derived from the GTOPO30 dataset. An area-true interpolation to the Gaussian grid is used.

8.1.3 codes: 1740, 1741, 174

The data were provided by Diana Rechid, MPI Hamburg, as global fields with 0.5° resolution. A description on the method is available at [Rechid et al. (2009)] and [Rechid et al. (2008)]. The values refer to the land part of the grid box. They base on MODIS satellite data of the years 2001-2004 and do not represent land use change.
The soil albedo and the vegetation albedo are given as one yearly field. The albedo (code 174) is calculated from those two parts and from the monthly mean values of lai (code 200) to get a yearly cycle.

8.1.4 codes: 169, 210

The sea ice cover and the surface temperature are calculated from the AMIP-II boundary condition dataset (`http://www-pcmdi.llnl.gov/projects/amip`) as multi year monthly mean values over the whole time period (1870-2006). The surface temperature is given in AMIP-II as sea surface temperature which is also defined for land points in order to enable land sea mask modifications without changing the SST field. The data were provided by Karl Taylor, PCMDI, on Gaussian grid in resolutions T21, T31 and T42.

8.2 Modification

The fields described above (except codes 129, 172, 169 and 210) are composed of useful values on land points and missing values or dummy values on sea points. The land sea mask of the data does not match the (currently) used land sea mask of PlaSim exactly, and probably the PlaSim land sea mask will be changed slightly for some simulations. To avoid the problem that some land points might not get proper values of surface data, we decided to extend the land point values to the sea points.
This is done as follows:
All gridpoints with:

value .lt. 0.0001 .AND. lsm .le. 0.005

are considered as changeable sea points.

The *value* is replaced by the *value* of the left and/or right neighboring point. Therefore the neighboring point has to meet the requirements:

value .ge. 0.0001 .OR. lsm .gt. 0.005

If only one neighboring point fulfills this condition, the value is taken,
if both neighboring points fulfill this condition, the average of their values is taken,
if no neighboring point fulfills this condition, the value stays unchanged until the next iteration.

ATTENTION: For this reason the resulting fields have to be modified by the used land sea mask to mask out the values on sea points!!!

Additions / Exceptions:

1. lower limit for z0 (code 173) and z0t (code 1730) is set to 0.0001m
2. lower limit for "Maximum soil water holding (field) capacity" (code 229) is set to 0.001m, units are set to [m] (from [mm]).
3. threshold value (for gridpoints to change, see above) for z0 (code 173) and albedo (codes 1740,1741,174) is set to 0.5 instead of 0.005
4. only for T31-fields: for vegc (code 199) and lai (code 200), the threshold value for lsm is set to 0.5 instead of 0.005

8.3 Examples

As an example the fields in T21 resolution are shown. For sg, tsa, lsm and sic the whole fields are plotted, for all other fields only gridpoints with lsm > 0.005, which are considered as land points.
For alb, vegc, lai, tsa and sic the fields of January and July are shown.

land sea mask [fract.]
code 172

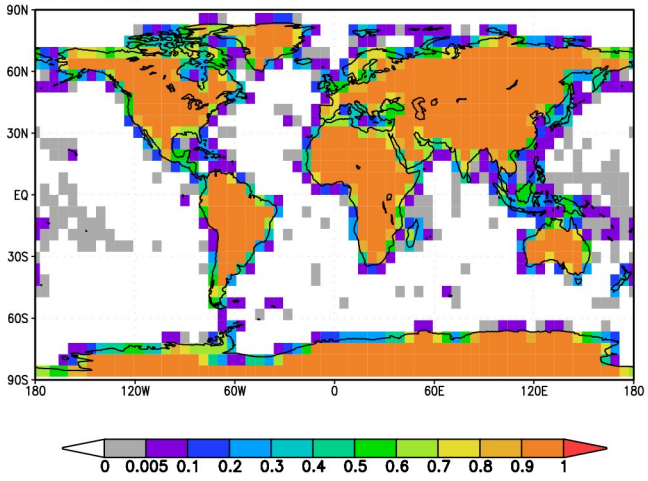

orography [m]
code 129

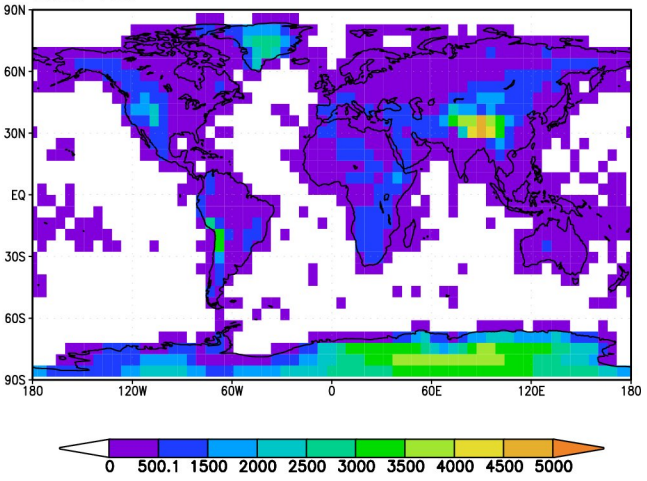

surface temperature accumulated [°C] Jan
code 169

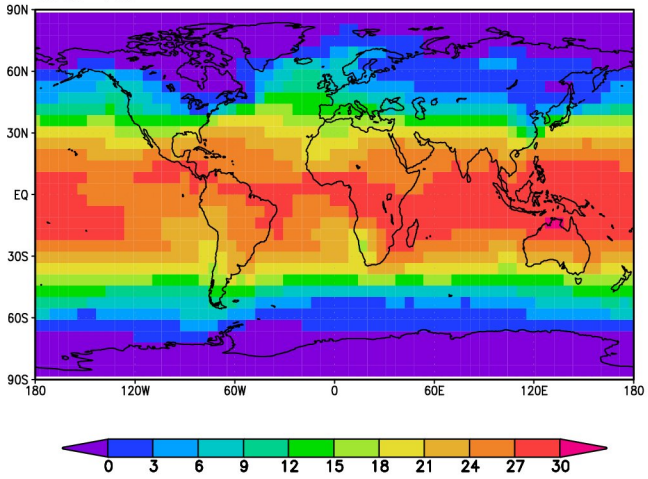

surface temperature accumulated [°C] Jul
code 169

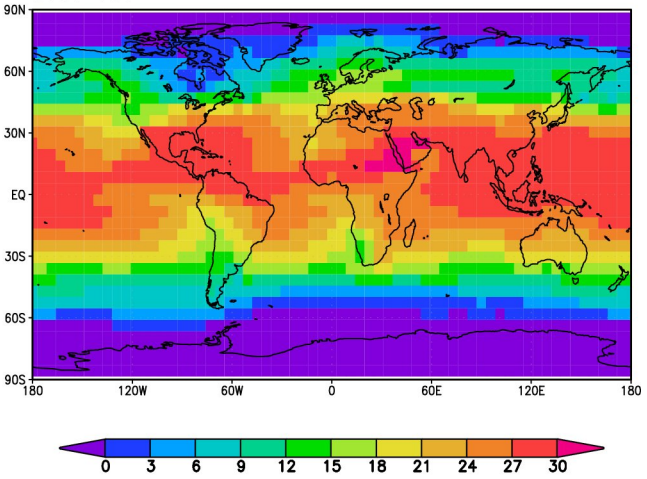

sea ice cover [%] Jan
code 210

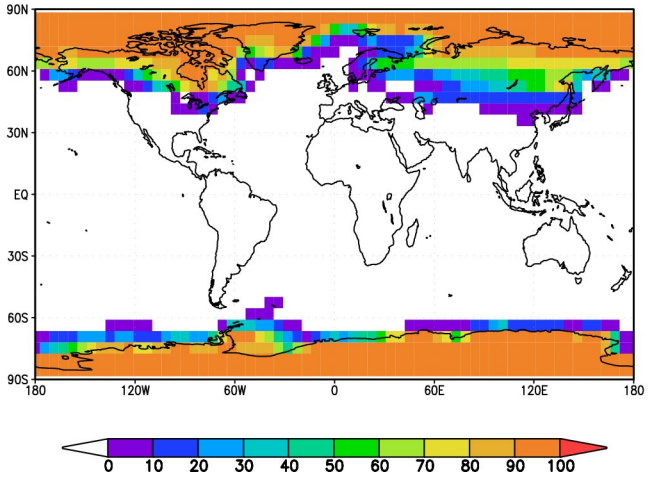

sea ice cover [%] Jul
code 210

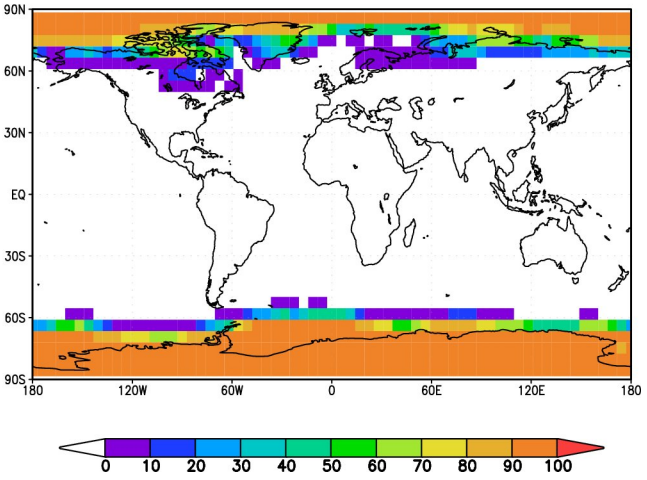

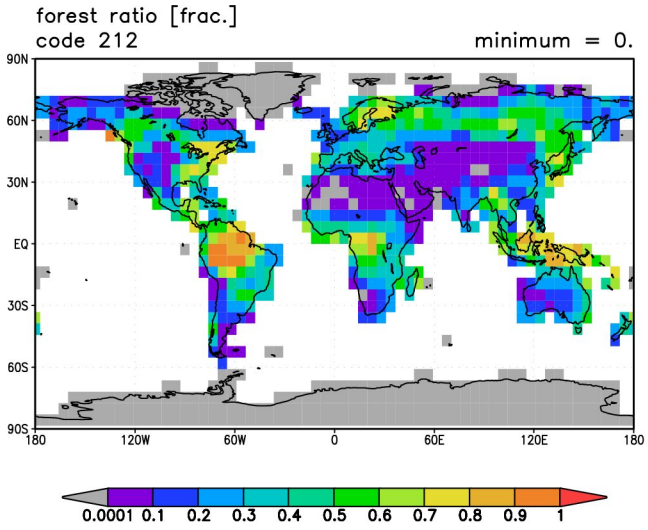
forest ratio [frac.]
code 212
minimum = 0.
90N
60N
30N
EQ
30S
60S
90S
180
120W
60W
0
60E
120E
180
0.0001 0.1 0.2 0.3 0.4 0.5 0.6 0.7 0.8 0.9 1

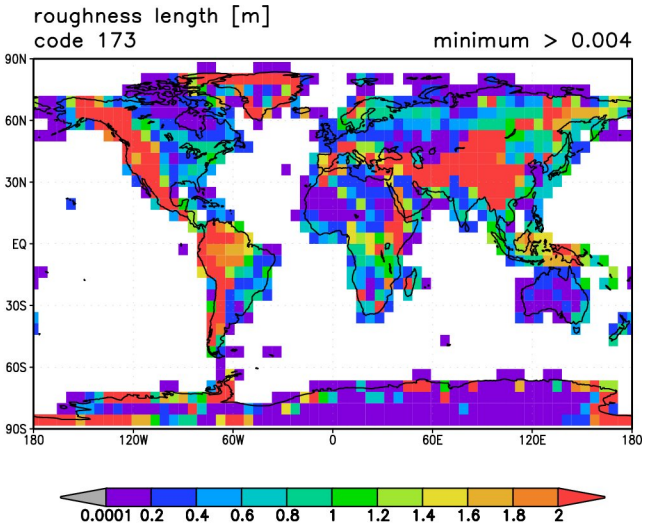
roughness length [m]
code 173
minimum > 0.004
90N
60N
30N
EQ
30S
60S
90S
180
120W
60W
0
60E
120E
180
0.0001 0.2 0.4 0.6 0.8 1 1.2 1.4 1.6 1.8 2

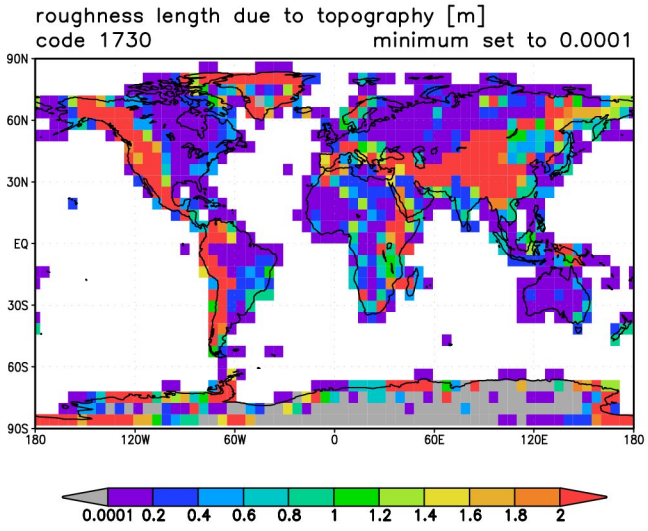
roughness length due to topography [m]
code 1730
minimum set to 0.0001
90N
60N
30N
EQ
30S
60S
90S
180
120W
60W
0
60E
120E
180
0.0001 0.2 0.4 0.6 0.8 1 1.2 1.4 1.6 1.8 2

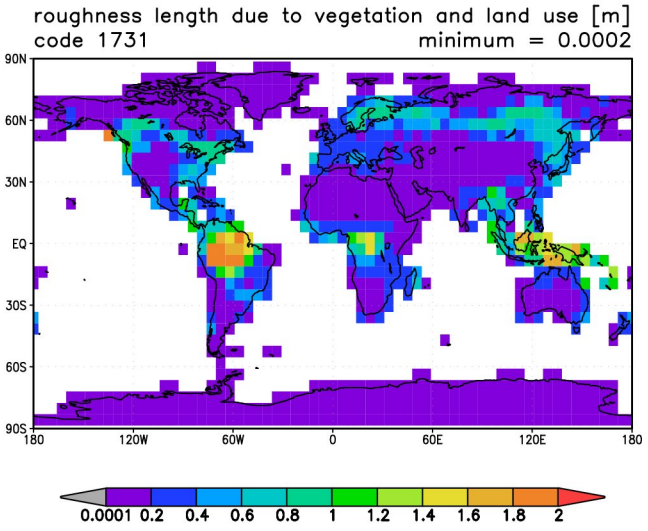
roughness length due to vegetation and land use [m]
code 1731
minimum = 0.0002
90N
60N
30N
EQ
30S
60S
90S
180
120W
60W
0
60E
120E
180
0.0001 0.2 0.4 0.6 0.8 1 1.2 1.4 1.6 1.8 2

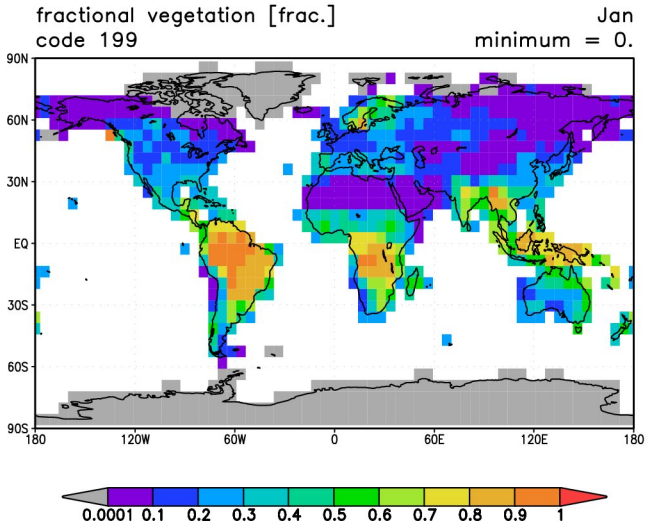
fractional vegetation [frac.]
Jan
code 199
minimum = 0.
90N
60N
30N
EQ
30S
60S
90S
180
120W
60W
0
60E
120E
180
0.0001 0.1 0.2 0.3 0.4 0.5 0.6 0.7 0.8 0.9 1

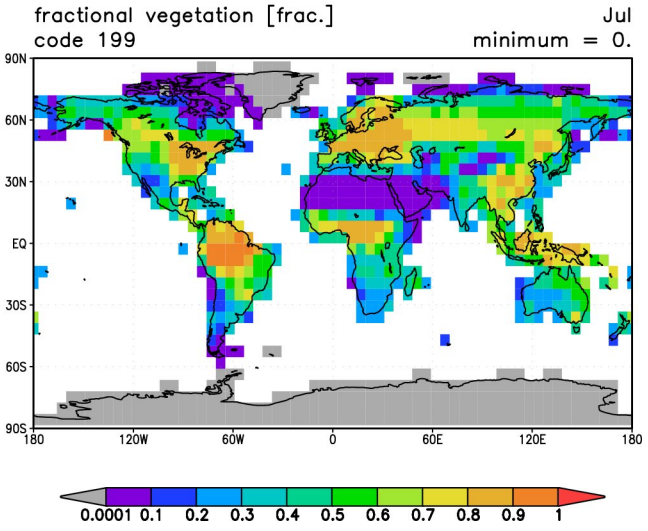
fractional vegetation [frac.]
Jul
code 199
minimum = 0.
90N
60N
30N
EQ
30S
60S
90S
180
120W
60W
0
60E
120E
180
0.0001 0.1 0.2 0.3 0.4 0.5 0.6 0.7 0.8 0.9 1

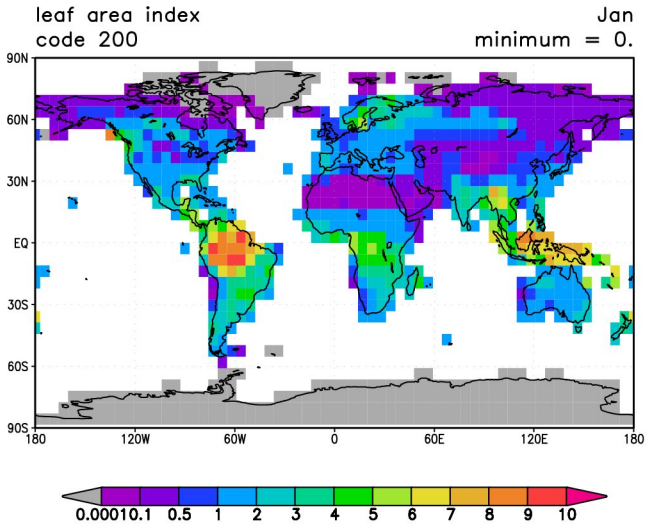
leaf area index
code 200
Jan
minimum = 0.
90N
60N
30N
EQ
30S
60S
90S
180
120W
60W
0
60E
120E
180
0.00010.1 0.5 1 2 3 4 5 6 7 8 9 10

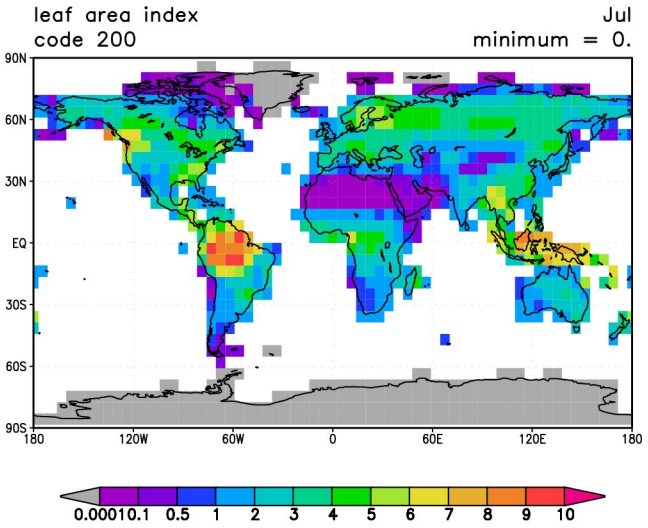
leaf area index
code 200
Jul
minimum = 0.
90N
60N
30N
EQ
30S
60S
90S
180
120W
60W
0
60E
120E
180
0.00010.1 0.5 1 2 3 4 5 6 7 8 9 10

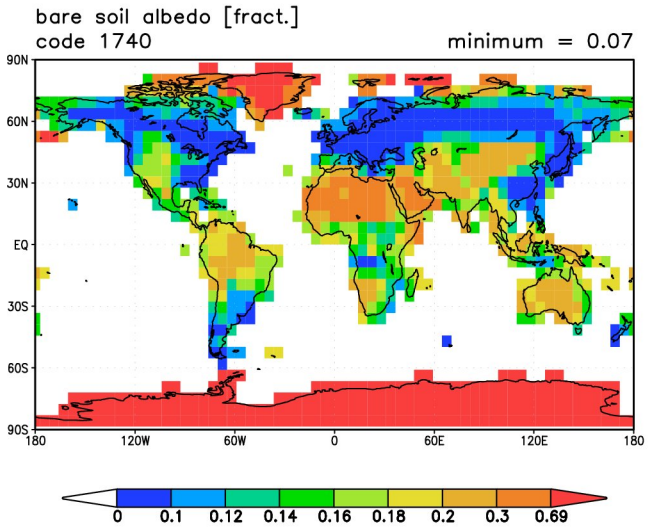
bare soil albedo [fract.]
code 1740
minimum = 0.07
90N
60N
30N
EQ
30S
60S
90S
180
120W
60W
0
60E
120E
180
0 0.1 0.12 0.14 0.16 0.18 0.2 0.3 0.69

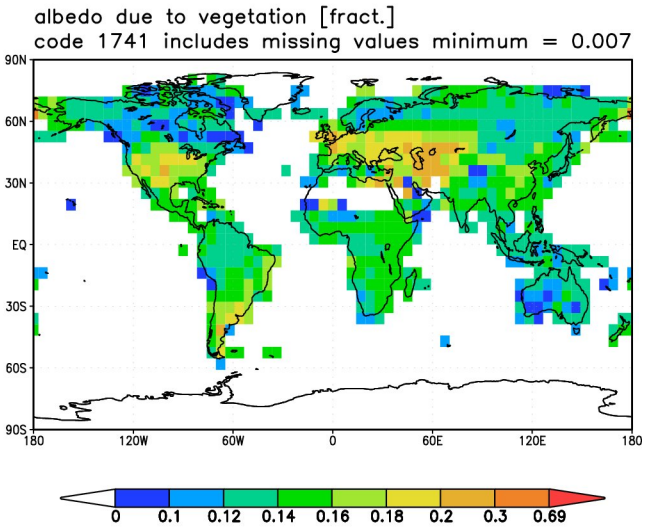
albedo due to vegetation [fract.]
code 1741 includes missing values minimum = 0.007
90N
60N
30N
EQ
30S
60S
90S
180
120W
60W
0
60E
120E
180
0 0.1 0.12 0.14 0.16 0.18 0.2 0.3 0.69

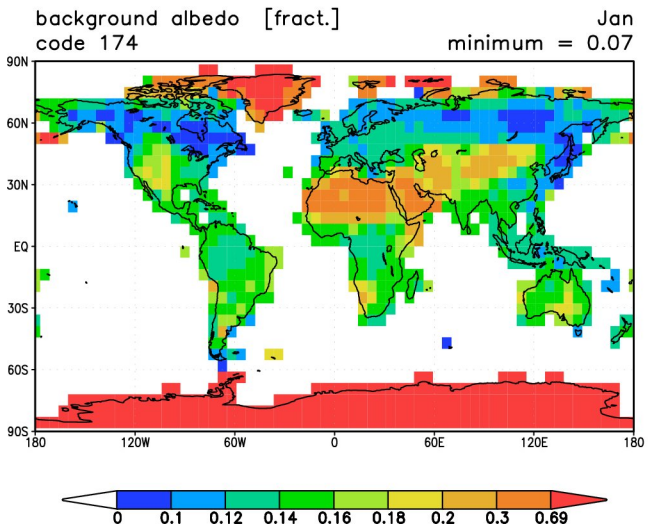
background albedo [fract.]
code 174
Jan
minimum = 0.07
90N
60N
30N
EQ
30S
60S
90S
180
120W
60W
0
60E
120E
180
0 0.1 0.12 0.14 0.16 0.18 0.2 0.3 0.69

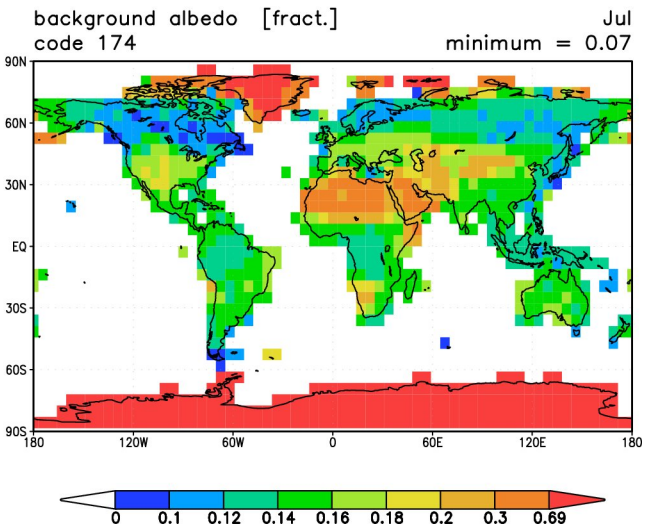
background albedo [fract.]
code 174
Jul
minimum = 0.07
90N
60N
30N
EQ
30S
60S
90S
180
120W
60W
0
60E
120E
180
0 0.1 0.12 0.14 0.16 0.18 0.2 0.3 0.69

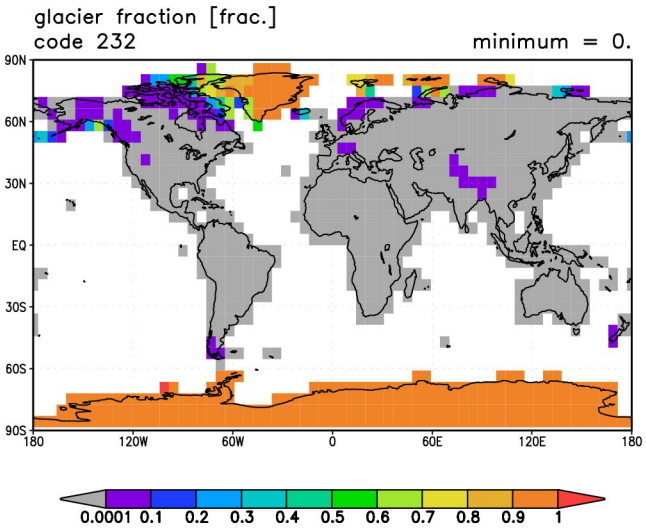
glacier fraction [frac.]
code 232
minimum = 0.
90N
60N
30N
EQ
30S
60S
90S
180
120W
60W
0
60E
120E
180
0.0001 0.1 0.2 0.3 0.4 0.5 0.6 0.7 0.8 0.9 1

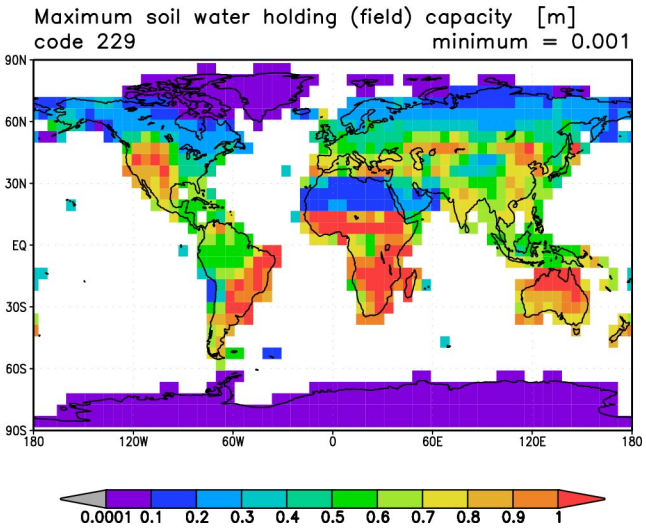
Maximum soil water holding (field) capacity [m]
code 229
minimum = 0.001
90N
60N
30N
EQ
30S
60S
90S
180
120W
60W
0
60E
120E
180
0.0001 0.1 0.2 0.3 0.4 0.5 0.6 0.7 0.8 0.9 1

Part VI

Bibliography

Bibliography

[Albertson and Kiely (2001)] Albertson, J. D., G. Kiely, On the structure of soil moisture time series in the context of land surface models, *Journal of Hydrology*, **243**, 101–119, 2001.

[Apel (1987)] Apel, J. R., Principles of Ocean Physics, *Academic Press*, Int. Geophys. Ser., **38**, 1987.

[Beckmann and Birnbaum (2001)] Beckmann, A. and Birnbaum, G., Cryosphere : Coupled Sea Ice - Ocean Models, *Academic Press*, Encyclopedia of Ocean Sciences, 2001.

[Betts and Ball (1997)] Betts, A. K. and J. H. Ball, Albedo over the boreal forest, *Journal of Geophysical Research*, bf 102(D24), 28901-28909, 1997.

[Birnbaum (1998)] Numerical modelling of the interaction between atmosphere and sea ice in the Arctic marginal ice zone, *Alfred Wegener Institute for Polar and Marine Research*, PhD-thesis, 1998.

[Bliss et al. (1981)] Bliss LC, Heal OW, Moore JJ (eds) (1981) Tundra ecosystems: a comparative analysis. Cambridge University Press, Cambridge.

[Buizza et al. (1999)] Buizza, R., Miller, M. and Palmer, T. N., Stochastic representation of model uncertainties in the ECMWF Ensemble Prediction System, *Q. J. R. Meteorol. Soc.*, **125**, 2887–2908, 1999.

[Brooks et al. (1997)] Brooks JR, Flanagan LB, Varney GT, Ehleringer JR, Vertical gradients of photosynthetic gas exchange and refixation of respired CO2 withini boreal forest canopies, *Tree Physiol*,**17**, 1–12, 1997.

[Bunce (2005)] Bunce, J. A., What is the usual internal carbon dioxide concentration in C4 species under midday field conditions? *Photosynthetica*, **43**, 603-608, 2005.

[Cattle and Crossley (1995)] Cattle, H. and Crossley, J., Modelling Arctic Climate Change, *Phil. Trans. Roy. Soc. Lon. A*, **352**, 201–213, 1995.

[Cox et al. (1999)] Cox PM, Betts RA, Bunton CB, Essery RLH, Rowntree PR, Smith J, The impact of new land surface physics on the GCM simulation of climate and climate sensitivity, *Clim Dyn*, bf 15, 183–203.

[Cramer et al. (1999)] Cramer W, Kicklighter DW, Bondeau A et al., Comparing global models of terrestrial net primary productivity (NPP): Overview and key results. *Global Change Biology*, **5** (Supplement 1), 1–15, 1999.

[DeLucia et al. (2007)] Delucia, E.H., Drake, J.E., Thomas, R.B. and Gozalez-Meler, M., Forest carbon use effciency: is respiration a constant fraction of gross primary production? *Global Change Biology*, **13**, 1157–1167, 2007.

[Dewar (1997)] Dewar, R. C., 1997, A simple model of light and water use efciency for pinus radiata, *Tree Physiology*, **17**, 259–265, 2007.

[Dommenget and Latif (2000)] Dommenget, D. and Latif, M., Generation of SST anomalies in the midlatitudes, *Max-Planck-Institut Report*, **304**, 2000.

[Eliassen et al. (1970)] Eliassen, E., Machenhauer, B., and Rasmusson, E., On a numerical method for integration of the hydrodynamical equations with a spectral representaion of the horizontal fields, *Inst. of Theor. Met., Univ. Copenhagen*, 1970.

[Field et al. (1995)] Field, C. B., J. T. Randerson, and C. M. Malmstrom, Global net primary production: Combining ecology and remote sensing, *Remote Sens. Environ.*, **51**, 74–88, 1995.

[Gao et al. (2005)] Gao, F., C. B. Schaaf, A. H. Strahler, A. Roesch, W. Lucht, and R. Dickinson, 2005: MODIS bidirectional reflectance distribution function and albedo Climate Modeling Grid products and the variability of albedo for major global vegetation types, *J. Geophys. Res.*, **110**, D01104, doi:10.1029/2004JD005190.

[García-Ojalvo and Sancho (1999)] García-Ojalvo, J. and Sancho, J. M., Noise in spatially extended systems, *Springer-Verlag, New-York*, 1999.

[Gaspar (1988)] Gaspar, P., Modeling the seasonal cycle of the upper ocean, *J. Phys. Oceanogr.*, **18**, 161–180, 1988.

[Gordon et al. (2000)] Gordon, C. et al. The simulation of SST, sea ice extents and ocean heat transports in a version of the Hadley Centre coupled model without flux adjustments, *Clim. Dyn.*, **16**, 147–168, 2000.

[Hagemann et al. (1999)] Hagemann, S., Botzet, M., Dümenil, L. and Machenhauer, B. Derivation of global GCM boundary layer conditions from 1 km land use satellite data *MPI Report, Max Planck Institute for Meteorology, Hamburg*, **289**, 1999.

[Hagemann (2002)] Hagemann, S., 2002 An improved land surface parameter dataset for global and regional climate models *MPI Report, Max Planck Institute for Meteorology, Hamburg*, **336**, 2002.

[Haltiner and Williams (1982)] Haltiner, G. J. and Williams, R. T., Numerical Prediction and Dynamic Meteorology, *John Wiley and Sons, New York*, 1982.

[Harvey (1989)] Harvey, L. D. D., 1989, Effect of model structure on the response of terrestrial biosphere models to CO2 and temperature increases, *Global Biogeochemical Cycles*, **3(2)**, 137–153, 1989.

[Hewitt (2000)] Hewitt, G., The genetic legacy of the Quaternary ice ages, *Nature*, **405**, 907–913, 2000.

[Hibler and Zhang (1993)] Hibler, W. D. III and Zhang, J. Interannual and climatic characteristics of an ice ocean circulation model, *Springer-Verlag New York*, NATO ASI Series Global and Environmental Change, 1993.

[Hoskins and Simmons (1975)] Hoskins, B. J. and Simmons, A. J., A multi-layer spectral method and the semi-implicit method, *Q. J. R. Meteorol. Soc.*, **101**, 637–655, 1975.

[Houtekamer and Derome (1995)] Houtekamer, P. L. and Derome, J., Methods for ensemble prediction, *Mon. Wea. Rev.*, **123**, 2181–2196, 1995.

[Houtekamer et al.(1996)] Houtekamer, P.L., Lefaivre, L., Derome, J., Ritchie, H. and Mitchell, H., A system simulation approach to ensemble prediction, *Mon. Wea. Rev.*, **124**, 1225–1242, 1996.

[Karaca and Müller (1991)] Karaca, M. and Müller, D., Mixed-layer dynamics and buoyancy transports, *Tellus*, **43**, 350–365, 1991.

[Kiehl et al. (1996)] Kiehl, J. T., Hack, J. J., Bonan, iG. B., Boville, iB. A., Briegleb, B. P., Williamson, D. L. and Rasch, P. J., Description of the NCAR Community Climate Model (CCM3), *National Centre for Atmospheric Research*, 1996.

[King and Turner (1997)] King, J. C. and Turner, J., Antarctic Meteorology and Climatology, *Cambridge University Press*, 1997.

[Kleidon (2006)] Kleidon A., The climate sensitivity to human appropriation of vegetation productivity and its thermodynamic characterization, *Glob Planet Change*, **54**, 109–127, 2006.

[Knorr (2000)] Knorr, W., Annual and interannual CO2 exchange of the terrestrial biosphere: Process based simulations and uncertainties, *Global Ecol Biogeogr*, bf 9, 225-252, 2000.

[Kraus (1967)] Kraus, E. B. and Turner, J. S., One-dimensional model of the seasonal thermocline II. The general theory and its consequences. *Tellus*, **19**, 98–105, 1967.

[Lohmann and Gerdes (1998)] Lohmann, G. and Gerdes, R., Sea Ice Effects on the Sensitivity of the Thermohaline, *J. Clim.*, **11**, 2789–2803, 1998.

[Lorenzo and Pérez-Muñuzuri (1999)] Lorenzo, M. N. and Pérez-Muñuzuri, V., Colored noise-induced chaotic array synchronization, *Phys. Rev. E*, **60**, 2779–2787, 1999.

[Lorenzo and Pérez-Muñuzuri(2001)] Lorenzo, M.N. and Pérez-Muñuzuri, V., Influence of low intensity noise on assemblies of diffusively coupled chaotic cells, *Chaos*, *11*, 371–376, 2001.

[Lorenzo et al.(2002)] Lorenzo, M.N., Santos M.A. and Pérez-Muñuzuri, V., Spatiotemporal stochastic forcing effects in an ensemble consisting of arrays of diffusively coupled Lorenz cells, *submitted to Phys. Rev. E*, 2002.

[Lunkeit(2001)] Lunkeit, F., Synchronization experiments with an atmospheric global circulation model, *Chaos*, *11*, 47–51, 2001.

[McGuire et al. (1992)] McGuire, A. D., J. M. Melillo, L. M. Joyce, D. M. Kicklighter, A. L. Grace, B. Moore III, and C. J. Vorosmarty, Interactions between carbon and nitrogen dynamics in estimating net primary productivity for potential vegetation in North America, *Global Biogeochem. Cycles*, **6**, 101–124, 1992.

[Molteni et al.(1996)] Molteni, F., Buizza, R., Palmer T.N. and Petroliagis, T., The ECMWF ensemble prediction system: Methodology and validation, *Q.J.R. Meteorol. Soc.*, *122*, 73–120, 1996.

[Monteith et al. (1989)] Monteith, J.L., A.K.S. Huda, and D. Midya. 1989. RESCAP: a resource capture model for sorghum and pearl millet. In *Modelling the Growth and Development of Sorghum and Pearl Millet*, Eds. S.M. Virmani, H.L.S. Tandon, and G. Alagarswamy. ICRISAT Research Bulletin 12, Patancheru, India, pp 30–34.

[Morison and Gifford (1983)] Morison J.I.L. and Gifford R.M., Stomatal sensitivity to carbon dioxide and humidity, *Plant Physiology*, bf 71, 789–796, 1983.

[Orszag (1970)] Orszag, S. A., Transform method for calculation of vector coupled sums, *J. Atmos. Sci.*, **27,** 890-895.

[Parkinson and Washington (1979)] Parkinson, C. L. and Washington, W. M., A large-scale numerical model of sea ice, *J. Geophys. Res.*, **84**, 311–337, 1979.

[Phillips (1957)] Phillips, N. A., A coordinate system having some special advatages for numerical forecasting, *J. Meteorology*, **14**, 184–185, 1957.

[Polley et al. (1993)] Polley, H.W., H.B. Johnson, B.D. Marino and H.S. Mayeux, Increase in C3 plant water-use efficiency and biomass over Glacial to present CO2 concentrations, *Nature*, **361**, 61–64, 1993.

[Potter et al. (1993)] Potter CS, Randerson J, Field CB, Matson PA, Vitousek PM, Mooney HA, Klooster SA., Terrestrial ecosystem production: a process model based on global satellite and surface data, *Global Biogeochemical Cycles*, **7**,811–841, 1993.

[Rechid et al. (2008)] Rechid, D., Hagemann, S., Jacob, D., Sensitivity of climate models to seasonal variability of snow-free land surface albedo. *Theor Appl Climatol, DOI 10.1007/s00704-007-0371-8*, 2008

[Rechid et al. (2009)] Rechid, D., T. J. Raddatz, D. Jacob, Parameterization of snow-free land surface albedo as a function of vegetation phenology based on MODIS data and applied in climate modelling, *Theor Appl Climatol*, **95**, 245–255, 2009.

[Roesch and Roeckner (2006)] Roesch, A. and E. Roeckner, Assessment of Snow Cover and Surface Albedo in the ECHAM5 General Circulation Model, *Journal of Climate*, **19**, 3828–3843, 2006.

[Roesch et al. (2001)] Roesch, A., M. Wild, H. Gilgen, A. Ohmura, A new snow cover fraction parametrization for the ECHAM4 GCM, *Climate Dynamics*, **17**, 933-946, 2001.

[Santos and Sancho(2001)] Santos, M.A. and Sancho, J.M., Front dynamics in the presence of spatiotemporal noises, *Phys. Rev. E*, *64*, 016129(1)–016129(11), 2001.

[Semtner (1976)] Semtner, A. J. Jr., A Model for the Thermodynamic Growth of Sea Ice in Numerical Investigations of Climate, *J. Physic. Oceanogr.*, **3**, 379–389, 1976.

[Simmons et al.(1978)] Simmons, A. J., B. J. Hoskins, and D. M. Burridge, 1978: Stability of the semi-implicit method of time integration. *Mon. Wea. Rew.*, **106,** 405–412.

[Simmons and Burridge (1981)] Simmons, A. J., and D. M. Burridge, 1981: An Energy and Angular-Momentum Conserving Vertical Finite-Difference Scheme and Hybrid Vertical Coordinates. *Mon. Wea. Rew.*, **109,** 758–766.

[Smith et al.(1999)] Smith, L.A., Ziehmann, C. and Fraedrich, K., Uncertainty dynamics and predictability in chaotic systems, *Q.J.R. Meteorol. Soc.*, *125*, 2855–2886, 1999.

[Tibaldi and Geleyn, (1981)] Tibaldi, S., and J.-F. Geleyn, The production of a new orography, land-sea mask and associated climatological surface fields for operational purposes *ECMWF Technical Memorandum*, **40** 1981.

[Timmermann (2000)] Timmermann, R., Wechselwirkungen zwischen Eis und Ozean im Weddelmeer, *University of Bremen*, 2000.

[Toth and Kalnay(1993)] Toth, Z. and Kalnay, E., Ensemble forecasting at NMC: The generation of perturbations, *Bull. Amer. Meteor. Soc.*, *74*, 2317–2330, 1993.

[Turnbull et al. (2002)] Turnbull, M.H., D. Whitehead, D. T. Tissue, W. S. F. Schuster, K. J. Brown, V. C. Engel, K. L. Griffin, Photosynthetic characteristics in canopies of Quercus rubra, Quercus prinus and Acer rubrum differ in response to soil water availability, *Oecologia*, bf 130, 515–524, 2002.

[UNESCO (1978)] Eighth report of the joint panel on oceanographic tables and standards, *UNESCO Technical Papers in Marine Science*, **28**, 1978.

[Whitaker and Lougue(1998)] Whitaker, J.S. and Lougue, A.F., The relationship between ensemble spread and ensemble mean skill, *Mon. Wea. Rev.*, *126*, 3292–3302, 1998.

[Wilks(1995)] Wilks, D.S., *Statistical methods in the atmospheric sciences*, Academic Press, New-York, 1995.

[Williamson et al. (2006)] Williamson, M. S., T.M. Lenton, J.G. Shepherd, N.R. Edwards, An effcient numerical terrestrial scheme (ENTS) for Earth system modelling, *Ecological Modelling*, **198**, 362–374, 2006.

[Wong et al. (1979)] Wong, S.C., I. R. Cowan, and G. D. Farquhar, Stomatal conductance correlates with photosynthetic capacity, *Nature*, **282**, 424–426, 1979.

[Yuan et al. (2007)] Yuan, W. and coauthors, Global pattern of NPP to GPP ratio derived from MODIS data: effects of ecosystem type, geographical location and climate, *Global Ecology and Biogeography*, **18**, 280–290, 2007.

[Zhang et al. (2009)] Zhang, Y., M. Xu, H. Chen, J. Adams, Deriving a light use effciency model from eddy covariance flux